Report

03ET7087E

Project: FlexGen – Innovations for the development of turbo generators for the support of the energy revolution
Subproject: Computer-aided prediction and optimization of the thermal and mechanical properties of novel composite materials for generator components with special focus on strength- and endurance-relevant properties[1]

Subproject leader: Prof. Dr.-Ing. Stephan Wulfinghoff, Institute for Materials Science, Christian-Albrechts-Universität zu Kiel

Project time: 01.04.2017 – 31.03.2021

Gefördert durch:

Bundesministerium für Wirtschaft und Energie

aufgrund eines Beschlusses des Deutschen Bundestages

The project on which this report is based was funded by the Federal Ministry for Economic Affairs and Energy under grant number 03ET7087E. The author is responsible for the content of this publication.

Das diesem Bericht zugrunde liegende Vorhaben wurde mit Mitteln des Bundesministeriums für Wirtschaft und Energie unter dem Förderkennzeichen 03ET7087E gefördert. Die Verantwortung für den Inhalt dieser Veröffentlichung liegt beim Autor.

---

1 German title: Innovationen zur Entwicklung von Turbogeneratoren zur Unterstützung der Energiewende; Teilvorhaben: Computergestützte Vorhersage und Optimierung der thermomechanischen Eigenschaften von neuartigen Verbundwerkstoffen für Generatorkomponenten mit besonderem Fokus auf festigkeits- sowie lebensdauerrelevante Eigenschaften

Table of Contents

1. Project content and goal....8

1.1. Task....8

1.2 Preconditions of the project....9

1.3. Planning and process of the project....9

1.4. State of the art....10

1.4.1. Core-shell rubber particle modified epoxy....10

1.4.2. Carbon fiber-reinforced epoxy....10

1.4.3. Woven fiber composite....11

1.5. Cooperation with other partners....11

2. Computational models and methods....14

2.1. Core-shell rubber particle reinforced epoxy model....16

2.2. Carbon fiber-reinforced epoxy model....17

2.3. Woven glass-fiber-reinforced epoxy model....18

3. Simulations....19

3.1. Application of the model to core-shell-rubber nano-particle-reinforced epoxy....19

3.1.1. Particle concentration effect....19

3.1.2. Particle size effect investigation....21

3.1.3. Epoxy properties effects....22

3.1.4. Fracture behavior of core-shell nano-particle-modified epoxies....23

3.2. Application of the model to unidirectional carbon fiber-reinforced epoxy....25

3.2.1. Material properties calculation.....25

3.2.3. Fiber shape effect.....29

3.2.4. Matrix voids effect.....32

3.2.4.1. Porosity effect.....34

3.2.4.2. Void distribution effect.....35

3.2.4.3. Void size effect.....36

3.3. Application of the model to woven glass fiber-reinforced epoxy.....37

3.4. Thermal study.....40

3.4.1. Core-shell-rubber particle modified epoxy.....41

3.4.1.1. Effect of the particle volume fraction and size.....41

3.4.1.2. Effect of the particle distribution.....42

3.4.2. Carbon-fiber-reinforced epoxy.....44

3.4.2.1. Fiber diameter and volume fraction effect.....45

3.4.2.2.Fiber cross-section shape effect.....46

3.4.3. Woven fiber composites.....47

4. Conclusion.....49

5. Appropriateness of work, usability of results and publications.....55

5.1. Appropriateness of the work done.....55

5.2. Usability of results.....55

5.3. Publications related to the project.....56

References.....57

1. Project content and goal

This project report summarizes the work done at RWTH Aachen University and Kiel University during the ‘FlexGen’-project. Several passages in this document have been taken from Boussetta et al. (2021).

1.1. Task

While structural applications of composite materials are increasing in several engineering fields where high stiffness- and strength-to-weight ratios, long fatigue life, superior thermal properties are required, there is always room for optimization to ensure optimum performance especially when severe operational constraints are imposed, therefore composite structures are usually tailored, depending on specific objectives.

In particular, the enhancement of the thermal and mechanical properties of novel composite materials has always been of high interest for designers of turbo generator components with a special focus on properties relevant to strength and service life to meet future requirements imposed by the advancing integration of renewable energies and it is in this framework that the project FlexGen falls.

Indeed, being aware that the behavior of composite materials is significantly influenced by the underlying microstructure, this project aims to develop a favorable combination between the material microstructural parameters ensuring to obtain an profitable composite material in terms of performance. To reach this goal, a campaign of experimental and numerical tests has been conducted in this project.

The contribution of our group in the framework of the project manifests itself in the development of a microscale numerical study aiming at a quick and cost-effective prediction of the overall thermal and mechanical properties of the composite materials of the generator components for different microstructures which would allow afterwards their improvement. Indeed, a geometrically nonlinear elastoplastic gradient-enhanced damage model with incremental potential has been developed and applied to composite materials of the generator components such as brittle woven composites, particle reinforced plastics, and unidirectional fiber-reinforced composites.

The approach followed to achieve the overall purpose depicted above could be divided into three key steps:

1. Provide an insight into the microscopic failure behavior of the composite materials using adaptive meshing to enable a refined numerical resolution of cracked regions.
2. Investigate the influence of microstructural and material parameters on the overall composite material behavior and find favorable values for these parameters.

3. Evaluate and validate the efficiency of the model developed in simulating the behavior of such complex material structures by referring to the literature and the experimental results.

1.2 Preconditions of the project

The expansion of renewable energies in the context of the energy transition cannot be viewed separately from the use of conventional energy generation. As a result of the increasing share of renewable energies, the mode of operation of conventional power plants is also changing, which increasingly have to compensate for the fluctuating availability of renewable energies. The “FlexGen”-project focuses on generators, the changed mode of operation of which leads to increasing loads on the materials used, which were not designed for such loads. The aim of the project is to develop appropriate composite materials and make them usable for generators in order to be able to withstand the increased loads. The development of new materials is seen as a prerequisite for the expansion of renewable energies to be compatible with existing conventional energy systems and for the international competitiveness of German companies and research institutes in the field of renewable energies to be further promoted.

1.3. Planning and process of the project

This sub-project started at RWTH Aachen University with Prof. Dr.-Ing. Stefanie Reese from the Institute of Applied Mechanics as an additional project leader. With the call of the second project leader, Dr.-Ing. Stephan Wulfinghoff, to the professorship of “Computational Materials Science”, the project moved to Kiel University in August 2018.

Table 1: Time schedule of the project (project-extension in yellow color)

	Tasks	1. Year				2. Year				3. Year				4. Year			
		1	2	3	4	1	2	3	4	1	2	3	4	1	2	3	4
1	Material model development																
2	Material param. identification																
3	Characterization of the micro-structural influence																
4	Improvement of mechanical and thermal properties																

The relocation to Kiel also had an impact on the project work, as the computational tools and infrastructure, which had been available in Aachen, first had to be reinstalled in Kiel. The research assistant working on the project changed as well. All these changes made the full processing of the goals of the project impossible before the set deadline. As a result, a cost-neutral project extension was conducted. Table 1 presents an overview of the time scheduled for each task of this sub-project before (grey) and after (yellow) extension.

1.4. State of the art

Epoxy resins are highly competitive among thermoset materials in industrial applications owing to their excellent thermal and chemical resistance as well as the high tensile strength and stiffness they exhibit. However, they suffer from a main drawback restricting their usage in many practical applications which is their limited resistance to the initiation and the growth of cracks. Therefore, researchers have become increasingly interested in the enhancement of the toughness of epoxy resins to ensure their reliability (Seymour, 1989). Several studies have been carried out for this purpose by the addition of a stiff or soft second phase to the resin (Garg and Mai, 1988).

A second phase used to improve the toughness of epoxies can be organic or inorganic. The latter is widely used for this purpose such as carbon and glass fibers. Soft reinforcing particles generally used are compliant rubbery particles. These two polymer toughening techniques were applied to obtain the materials of the generator components and will be more detailed in this section.

1.4.1. Core-shell rubber particle modified epoxy

The rubber-toughening technique includes two conventional methods. In the first one, the rubber is incorporated initially into the matrix as a miscible liquid, and then using a reactive additive, the second phase particles are formed. In this kind of compounds, the volume fraction and the size of the rubber particles are influenced by the degree of compatibility between the two phases and also the kinetics of gelation (Manzione et al., 1981) which makes the control of the compound morphology very difficult. This could be considered as a critical drawback as the fracture toughness of the compounds depends highly on the particle morphology (Bagheri et al., 2009). In the second method, the second phase is preformed and then included in the resin. This second phase is usally given in the form of core-shell particles with a rubbery core and a thin layer of a glassy shell. The rubbery core ensures the improvement of the toughness. The outer glassy shell is designed to be compatible with the resin, it improves the dispersion of the rubbery particles within the matrix and prevents their coalescence (Yee and Pearson, 1986).

The control of the particles' size and the volume fraction of the second phase is possible if core-shell particles are incorporated. This generation of modifiers is amongst the most preferred methods for the purpose of polymer toughening (Bagheri et al., 2009). This approach is also used as a for the optimization of materials in the framework of this project.

1.4.2. Carbon fiber-reinforced epoxy

The performance of FRP (fiber-reinforced polymer) composite materials predominantly depends on their constituent elements and manufacturing techniques. Therefore, various manufacturing techniques are used worldwide in the industry to fabricate optimized FRP composite materials for the desired application (Rajak et al. , 2019).

The filament winding is an automated composite fabrication technique competitive for the manufacturing of thick-walled components, such as the rotor cap in this project, enabling a fast production with few defects. This technique involves continuous winding of impregnated rovings of fibers in a resin bath just prior to application on a "winding-core" while keeping them in tension.

1.4.3. Woven fiber composite

The material of the insulation system of the generator stator investigated in this project involves in addition of the core-shell rubber particle modified epoxy composite, a woven glass fiber reinforced epoxy composite.

The manufacturing of the latter composite material consists of the continuous weaving of glass fiber rovings in two mutually perpendicular directions, which is subsequently embedded in epoxy resin. This composite provides bidirectional properties highly dependent on the weaving process parameters as well as the microstructural parameters of the reinforcing fibers such as the type, diameter, volume fraction and density.

1.5. Cooperation with other partners

Cooperation with other involved partners has been crucial. Indeed, important material parameters used in the numerical models developed have been identified experimentally and provided by other partners of the project. Furthermore, through regular virtual meetings and presentations a clear insight into the real materials behaviors has been provided which was extremely useful to depict these behaviors numerically. Indeed, without microscopic observations enabling to figure out damage phenomena that may appear in the materials of study being loaded, it wouldn’t be possible to predict and so simulate their failure behavior.

In return, the numerical results obtained in this project (and presented in this report) were communicated with the project partners in regular meetings and – with a larger audience – presented in the semi-annual project meetings. This regular communication of the results to the partners allowed them to develop an improved understanding of the micromechanical mechanisms which determine the behavior of the materials, which they developed and to better understand the results of their experimental investigations. This improved understanding fostered a knowledge-driven and goal-oriented development of the composite materials and an improved tailoring of the material properties towards the application in turbo generators. The details and results will be explained in the “Simulations”-section (sect. 3).

It is an experimentally proven fact, that testing the same type of composite material but with different microscopic geometrical parameters leads to different composite properties. A detailed understanding of this relation is a major goal of this project in order to identify favorable parameters based on microstuctural modifications.

Admittedly, experimental investigations could provide a clear overview of the effect of the microstructural parameters on the mechanical properties, however to quantify this effect experimentally and to find the best combination between parameters, leading to the best performance, would be extremely expensive in terms of money, time, and effort. And here manifests itself the requirement of the development of a computational tool in order to carry out such stochastic investigations, which was our task.

Table 2: Material properties of the epoxy matrix used to simulate the insulation system

Young's modulus E_e (Mpa)	Initial yield stress σ_{y0} (Mpa)	Elastic energy release rate g_c^e (J/m^2)	Poisson's ratio ν
3000	80	50	0.35

Table 3: Material properties of the carbon fiber reinforced epoxy composite material of the rotor cap

	Carbon fibers (diam=7um)	Epoxy
Volume fraction	60%	40%
Longitudinal Young's modulus	239000 (Mpa)	3030 (Mpa)
Transverse Young's modulus	15000 (Mpa)	--------
Longit. shear modulus	20000 (Mpa)	--------
Transverse shear modulus	6000 (Mpa)	--------
Longit. Poisson's ratio	0.2	0.35
Transverse Poisson's ratio	0.25	-------

For example, for the insulation system the requirements in terms of stiffness, strength, and toughness on the materials involved such as the CSRP (core-shell-rubber particles) modified epoxy and the woven fiber composite can only be fulfilled, if the microstructure is properly tailored. Using the computational models developed in this project, it is possible to choose the right microscopic properties of the reinforcing particles and rovings to be included in the epoxy resin in such a way that these requirements can be fulfilled. Similarly, for the CFRP (carbon fiber-reinforced plastic) material of the rotor cap, the shape, size, and volume fraction of the carbon fibers could be selected using, amongst other things, the outcome of our numerical study presented in the present report. The effect of voids, always present in the latter material, has been as well investigated numerically which could give an insight into acceptable and critical amounts of manufacturing defects.

Tables 2 and 3 gather typical mechanical properties used in the simulations presented in this report. It should be noted that the experimental characterization of the CFRP has been carried out on retaining rings obtained by winding rovings consisting of 24000 fibers with a diameter of 7µm of carbon fibers a priori impregnated in the epoxy. Concerning the properties of the components of the woven fiber composite considered to model its behavior, they are typical literature values and will be presented later (Table 4). The related material models are documented in Boussetta et al. (2021). There, a detailed interpretation of the parameters is given in terms of the detailed model equations.

2. Computational models and methods

The prediction of inelastic processes like plastic deformations and cracks within the microstructure of novel composite materials by realistic, yet simple and efficient continuum models remains a major task in material modeling. For this purpose, gradient-extended standard dissipative solids represent one of the most promising model classes, which is also applied in the framework of this project to achieve the aim of simulating the nonlinear elastoplastic behavior of the particle- and fiber-reinforced plastics investigated in the project. The applied models allow the prediction of the microscopic failure in these complex composite microstructures by the combination of a geometrically nonlinear elastoplastic model with an isotropic gradient-extended damage model to simulate microcracks.

A set of Fortran codes has been created and implemented within the framework of this project to accurately simulate the failure behavior of the materials of study. This includes, e.g., the implementation a remeshing tool with the aim to increase the numerical resolution in cracked regions (see Fig. 1). This local mesh refinement is necessary, since the computational times for the involved three-dimensional microstructures are generally high and a homogeneous mesh refinement (i.e., a refinement of the whole mesh) would be computationally too demanding to meet the project aim of a fast estimates of the overall composite properties. If refinement is needed, the simulation is executed two times: one time without refinement to locate regions with intense damage where refinement is needed and a second time with refined mesh based on the output of the first execution indicating where to refine. This process could be repeated a third and fourth time until the desired refinement level is reached.

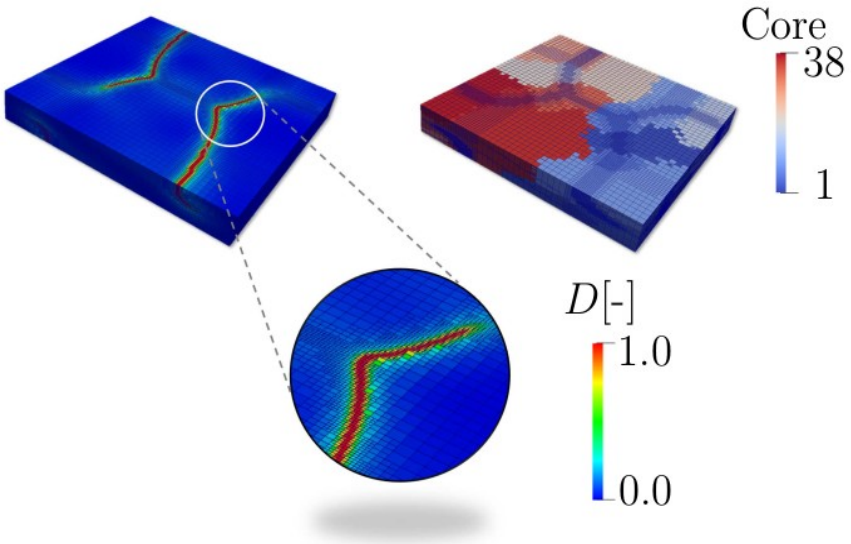

Figure 1: Left: Investigation of crack formation in terms of a damage variable D (cracks in red color) with adaptive remeshing algorithm. Right: Cores used in parallelized simulation.

Furthermore, it turned out that simulations on a single core are too time-consuming, such that the parallel version of the applied finite element software[2] had to be installed using the parallelization suite PETSc. The implementation of the remeshing algorithm and the parallelization weren't envisaged in the original project plan but turned out to be indispensable for the success of the project in order to perform the numerous three-dimensional highly nonlinear finite element simulations presented in the sequel. The extra time needed for the implementation was by far balanced by the computational time saved owing to these measures.

Figure 1 shows an exemplary section of the mesh adopted to investigate the failure behavior of a woven fiber composite. It can be clearly noticed that the mesh is refined only at regions of crack formation (damage variable D high) which are, inter alia, regions of intense stress concentration. The same figure also highlights the use of a parallel build (38 cores) with the aim of higher efficiency and faster simulations.

Computational modeling of composites with periodic microstructure can be performed by the consideration of a periodic unit cell of the material which is the smallest volume over which computation can be made leading to a representative response of the whole composite behavior. Therefore, for CFRP (carbon fiber-reinforced plastic), CSR (core-shell rubber) particle modified epoxy and woven glass fiber-reinforced epoxy, unit cell models have been set up to conduct all simulations to investigate the impact of different material and microstructural parameters on the behavior of the composites. Such unit cells should contain sufficient information about the reinforcing inclusions' (particles or fibers) size, volume fraction, type, orientation and spatial distribution.

Indeed, to reach the project goal of characterizing the influence of different microstructural and material parameters on the overall behavior of the materials, comparative studies have been carried out by the implementation of a Fortran code capable of incorporating inclusions of different shapes and sizes in the composite unit cell according to the distribution and the volume fraction desired. This code is updated from a microstructure to another based on the investigation needed for the materials. Exemplary finite element discretizations of microscopic unit cells modeled to simulate the behavior of the CSR particle modified epoxy, the carbon fiber-reinforced epoxy and the woven fiber-reinforced epoxy are shown, respectively, in Fig. 2a, b and c. For further information, see Boussetta et al. (2021).

Concerning the boundary conditions, a tensile loading has been imposed in terms of displacements on unit cells of the three microstructures. Trilinear hexahedral elements with reduced integration and hourglass stabilization have been used. Several material and finite element subroutines have been implemented based on a newly developed material model being capable to describe the elastoplastic geometrically nonlinear behavior of the materials involved (Boussetta et al., 2021). These subroutines have been adopted depending on the composite microstructure to be characterized. It should be mentioned, that the original project plan neither envisaged the usage of a geometrically nonlinear material model nor the incorporation of plastic material behavior. The

2 FEAP: Finite Element Analysis Program, Robert Taylor, Berkeley.

reason is that experimental tests performed with the composite materials suggest a rather brittle behavior, i.e., the material behavior is basically elastic until a crack forms in the specimen, leading to its more or less abrupt failure. Such type of behavior can be simulated using relatively simple small strain elastic material models with (gradient-extended) damage. However, during the project, it turned out that the material behavior on the micro- and nanoscale is significantly more complex as the strains on this level are often significantly larger (partially more than 50%) and involve intense elastoplastic deformations. For this reason, a geometrically nonlinear elastoplastic material model coupled with (gradient-extended) damage had to be developed and to be implemented as material subroutine (see Boussetta et al., 2021). Furthermore, this also required to adopt a geometrically nonlinear element subroutine being able to treat the nearly incompressible large elastoplastic deformations occuring on the microscopic scale. Luckily, this additional work was successful and led to the implementation of the aforementioned models and computer codes, which allowed to perform the demanding simulations, which were necessary to reach the project goal of characterizing the microscopic deformation behavior of the composite materials developed in the project.

Carbon fibers in the CFRP microstructure have been assumed to be transversally isotropic and the related five independent material constants are listed in Table 3. The epoxy matrix has been modeled as an isotropic elastoplastic solid for the microstructures. All simulations are executed by the finite element analysis software FEAP (Taylor, 2014) and use a parallel build (38 cores). Methodologies adopted to model reinforcing inclusions for the microstructures are illustrated in the following sections.

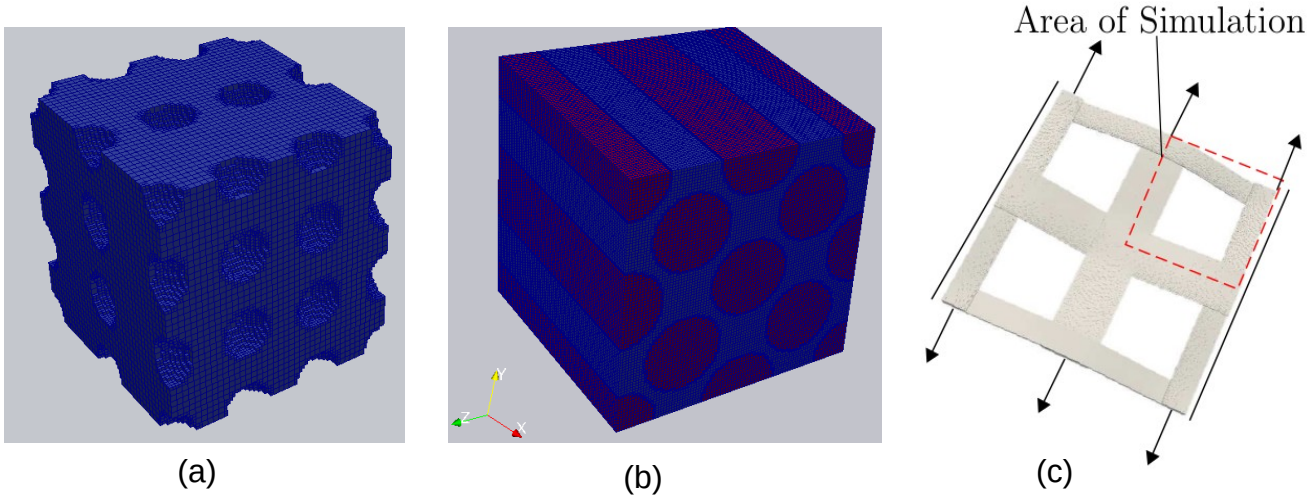

Figure 2: Material unit cells: (a) 0,5 µm×0,5 µm×0,5 µm cubic unit cell of epoxy modified with spherical CSR nano-particles (modeled as voids) of 50nm radius, (b) model of the CFRP microstructure with 60% of circular fibers, (c) model of the woven fiber composite under uniaxial tension and constrained transversal contraction.

2.1. Core-shell rubber particle reinforced epoxy model

Basically, '*toughening*' is the increase of the ability of the material to absorb energy during the fracture process. This is important, as a major goal of this project is to increase the resistance of the

turbo generator composite materials against fracture. The incorporation of rubbery particles in the epoxy resin involves the apparition of several dissipative mechanisms when the compound is loaded, such as shear banding in the epoxy matrix between the rubbery particles, the cavitation of the rubbery particles, the plastic deformation, the growth of the voids initiated by cavitation of the particles and the so-called “rubber-bridging” mechanism (Yee and Pearson, 1986; Huang and Kinloch, 1992; Giannakopoulos et al., 2011). Yee and Pearson (1986) reported that the particles’ cavitation is not only a dissipative mechanism but also the mechanism that triggers the whole toughening process. Indeed, the voids resulting from the cavitation of the rubber particles act as stress concentrators and relieve the triaxial stress state ahead of cracks. Therefore, the fracture of the compound is delayed by allowing the plastic void growth and the shear banding in the matrix instead.

As the particle-induced toughening is basically due to an increased amount of energy absorbed through the plastic growth of the voids and the shear yielding in the matrix between these voids, it is obvious to assume that the improvement of toughness depends highly on the volume fraction of the particles, on their size as well as their distribution in the matrix. The effects of these parameters on the behavior of the rubber-epoxy compounds are commonly examined by several experimental studies. The review made by Bagheri et al. (2009) outlines the most important findings of these investigations. In the same context, this study aims to characterize numerically the behavior of the epoxy being modified with rubbery particles for different microstructures and to use this information to develop favorable composite materials for the application in turbo generators.

It is obvious that a detailed model would ensure the identification of the various energy-dissipating mechanisms involved when rubbery nano-particles are added as well as the quantification of their contributions to the toughening to epoxy. However, as described, e.g. by Huang and Kinloch (1992) and Giannakopoulos et al. (2011), the plastic shear banding in the epoxy matrix and the plastic void growth are the main toughening mechanisms. These results justify the simplifying assumption that the cavitation mechanism can be neglected. Thus, the particles have been represented as spherical voids dispersed in the matrix. Moreover, it has been reported that rubber particles cavitate at a relatively low-stress level (Giannakopoulos et al., 2011) and have a stiffness much smaller than that of the surrounding polymer. This supports the assumption of the representation of the particles as voids. The same approach has been adopted in several studies (Smit et al., 1999; Steenbrink and Van der Giessen, 1999; Pijnenburg and Van der Giessen, 2001; Meijer and Govaert, 2003).

2.2. Carbon fiber-reinforced epoxy model

Despite the competitiveness of the filament winding technique, which is used in this project to produce CFRPs, the presence of manufacturing defects in the material is unavoidable. Voids are one of the most significant defects that could be generated during the manufacturing of CFRP composites which represent regions unfilled with polymer and fibers. Their significance is due to their high formation probability as well as to their considerable effect on mechanical composite properties and their contribution to the creation of new damage mechanisms leading to failure. As a result of their importance, voids are by far the most studied manufacturing defect.

A numerical model to highlight the effect of this defect on the behavior of the CFRP material has been set up by the incorporation of holes in different sizes and fractions in the unit cell model of the CFRP microstructure.

In contrast to the CSRP microstructure model the model of the CFRP involves the definition and the implementation of two materials, as shown in Fig. 2b. Indeed, unidirectional cylinders are included in the matrix in an hexagonal arrangement to model transversely isotropic carbon fibers. In addition to circular fibers, elliptical reinforcing fibers have been considered in order to investigate the effect of the fiber shape on the overall composite behavior. The volume fraction of the fibers has been as well varied to investigate its effect on the composite properties.

2.3. Woven glass-fiber-reinforced epoxy model

Simulations were performed to investigate the stress response and resistance to fracture of a woven structure of rovings embedded in a brittle matrix. Therefore, a displacement-controlled uniaxial tension test with one constrained and one free transversal contraction is performed on the three-dimensional modeled structure depicted in Fig. 2c. Material parameters of typical simulations are given in Table 4. Due to the exploitation of symmetries, only one-quarter of the structure is considered. Since on this scale, no significant plastic deformations are expected, an small strain brittle-damage model is applied.

Using this model, the influence of the rovings' vertical and lateral thickness on the overall woven composite has been investigated. This model helped also to characterize the effect of the mechanical properties of each component (rovings and matrix) on the failure behavior of the overall composite.

Table 4: Material properties of the epoxy matrix (M) and rovings (R) composnents of the woven fiber composite used to manufacture the insulation system

Young Modulus E_M (Mpa)	Young Modulus E_R(Mpa)	Elastic energy release rate g_c^e (J/m^2)	Poisson's ratio ν_M	Poisson's ratio ν_R
3039	63647	133	0.36	0.213

3. Simulations

3.1. Application of the model to core-shell-rubber nano-particle-reinforced epoxy

A major project goal was the formulation and investigation of a material model of the nano-particle-reinforced epoxy. For this purpose, a comparison of the mechanical responses of microscopic computational unit cells including voids with different volume fractions and different sizes has been carried out to investigate the effect of these microstructural parameters on the tensile behavior of the CSRP-modified epoxy.

Further numerical tensile tests considering different matrix properties and using the same unit cell (Fig. 2a) have been performed to check if this variation could improve the performance of such composites.

A central project goal was the study of the failure behavior of such material and the investigation of the extent to which this behavior is affected by a variation of the microstructural parameters. For this purpose another model has been developed which will be illustrated afterwards. All results obtained are shown and discussed below.

3.1.1. Particle concentration effect

To investigate the effect of the particle concentration on the mechanical properties of the modified matrix, spherical voids with 50 nm radius were included in an ordered arrangement in a unit cell with dimensions 0,5µm×0,5µm×0,5µm as shown in Fig. 2 a. For different volume fractions between 0% and 11%, the corresponding stress-strain relations, tensile strength σ_{max}, stiffness and dissipated energy are depicted in Fig. 3 respectively. The stress-strain diagrams in Fig. 3a show an observable difference in the tensile test response for different volume fractions of particles (modeled as voids). With increasing volume fraction the tensile strength and stiffness decrease as shown in Figs. 3b and 3d.

As explained above, it seems that the voids present in the matrix are subject to high stresses during the loading of the whole volume and their growth makes the microstructure absorb more energy before failure.

Furthermore, as shown in Fig. 3c, the amount of dissipated energy at the maximum stress increases with increasing number of particles. A larger dissipation means that the material absorbs more energy when being plastically deformed and thus indicates a larger toughness of the material. Therefore, it can be concluded that, in this sense, the toughness is maximized for a volume fraction approximately equal to 11% where the energy dissipated is doubled compared to the unmodified matrix. A comparison between calculated and measured (measurements were done by the project partners) stiffnesses and strengths has been as well performed, and as it is shown in Fig. 3b and Fig. 3d, a reasonable agreement has been found which confirms the accuracy of our model.

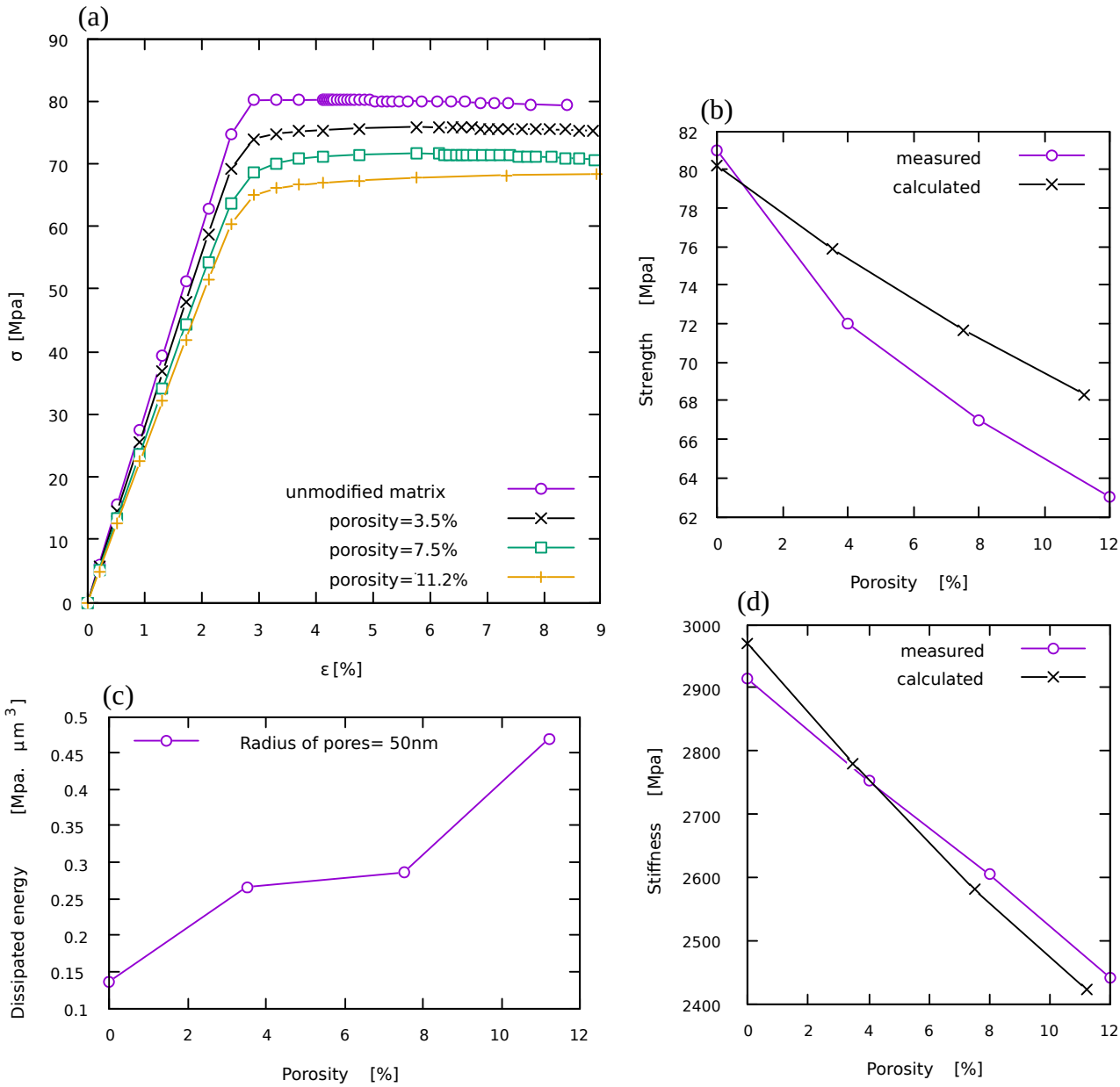

Figure 3: Effect of particle volume fraction on the (a) stress strain response under uniaxial loading, (b) maximum strength, (c) amount of disspated energy due to plastic deformation and (d) stiffness (Young's modulus). Here, 'porosity' refers to the void volume fraction in %.

3.1.2. Particle size effect investigation

For the investigation of nano-particle size effects on the modified matrix behavior, different volume fractions for particles with 25nm and 50nm radius were compared.

The resulting stress-strain diagrams for the 25nm particles and the comparison of dissipated energy for both sizes are given, respectively, in Fig. 4. The same effects as before can be seen with this model.

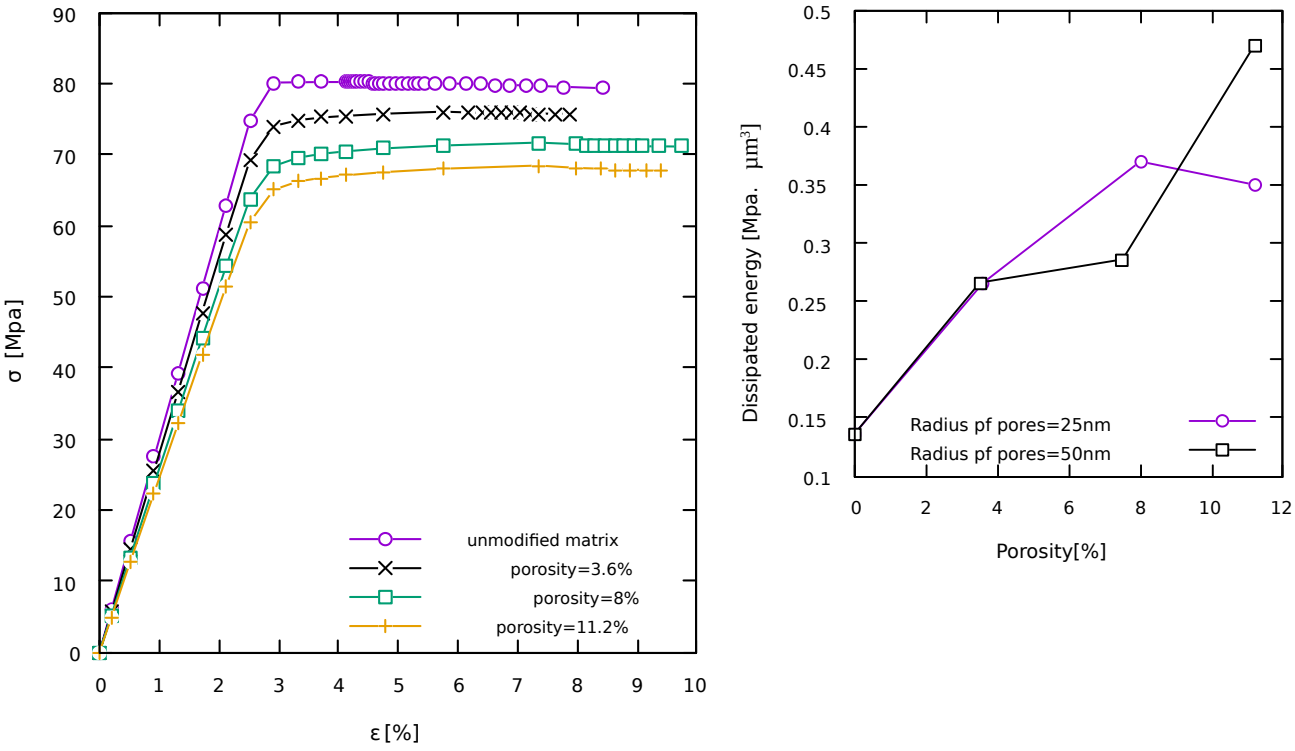

(a) (b)

Figure 4: Effect of the particle size: (a) Stress-strain response for different volume fractions of voids with radius 25nm included in 0,5μm×0,5μm×0,5μm cubic unit cell, (b) Comparison of dissipated energy for 25nm and 50nm particle size.

The maximum of energy dissipation for epoxy modified with particles of 25 nm radius is ensured at 8% of particle volume fraction. It can be further seen that the contribution to the dissipation is higher with the inclusion of particles with a radius of 50nm with a volume fraction of 11.2%.

3.1.3. Epoxy properties effects

The influence of the initial yield stress σ_{y0} and the elastic energy release rate g_c^e of the epoxy on the compound behavior was investigated by virtual tensile tests with a volume fraction of 8% and particle size (25nm). The corresponding stress-strain diagrams are given in Fig. 5.

As expected, Fig. 5a shows that a lower yield strength results in an earlier onset of plastic deformation. Therefore, up to a certain load level, the dissipated inelastic energy is greater with lower yield strength. However, at the maximum stress, the inelastic energy consumed is more important with higher yield strength.

The effect of the variation of the elastic energy release rate of the epoxy on the behavior of the material is illustrated in Fig. 5b. Indeed, up to ~10% strain, the different compounds with different values of g_c^e show the same behavior as well as the same dissipation of inelastic energy.

This can be explained by the fact that g_c^e is a fracture property while the initial deformation stage is entirely plasticity-dominated and the damage doesn't play a role initially.

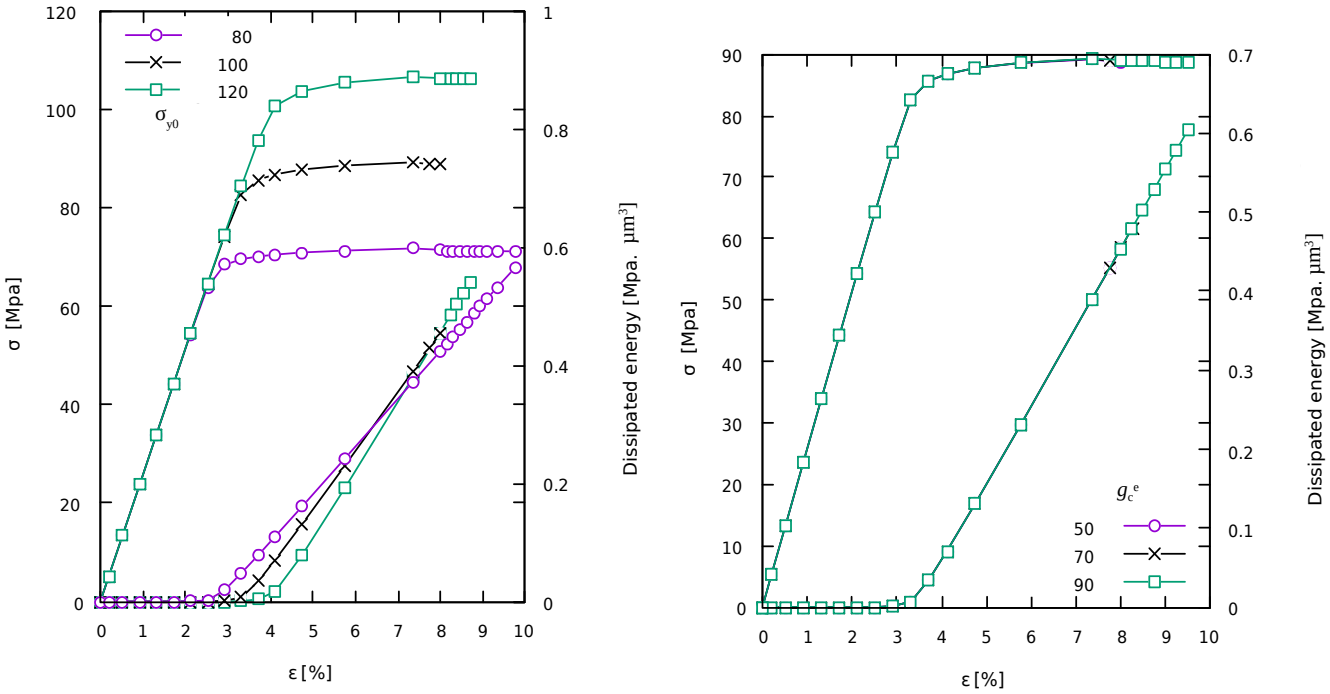

(a) (b)

Figure 5: Stress-strain response and amount of dissipated energy for different (a) initial yield stresses σ_{y0} and (b) elastic energy release rates g_{ce}

3.1.4. Fracture behavior of core-shell nano-particle-modified epoxies

Numerical simulations are typically performed in order to gain a better understanding of the material behavior and also to avoid difficult and expensive experiments. However, the numerical modeling of core-shell particle-modified polymers is still in a rather early stage due to the complexity of the fracture behavior of this type of materials.

In this section, a numerical attempt to investigate the effect of the core-shell particles, being again modeled as voids, on the fracture behavior of the modified epoxy is presented. While the investigation of the toughness can be measured roughly by the consideration of the area under the stress-strain curve obtained through the tensile loading of an assumed perfect material, the identification of measures related to the fracture toughness, defined by the ability of the material with cracks to resist fracture by absorbing energy, requires the consideration of a precrack.

Therefore, to investigate the effect resulting from the addition of core-shell particles to the matrix on the compound fracture toughness, a precrack has been considered in the model of the material, and only the process zone ahead of the crack tip has been modeled. Besides the enormous computational effort that would be needed to model the entire microstructure, the modeling of the crack tip is also motivated by the fact that in the presence of a crack, the dissipative mechanisms such as the shear banding in the epoxy are enabled by the plastic growth of the voids subjected to the high triaxial loads prevailing only ahead of the crack tip.

Mode I loading has been considered in this model to investigate the resistance of the material against crack growth. Therefore a displacement has been imposed at the top of the microstructure and lateral contractions have been restricted. Due to the symmetry of the model only a part of the problem has been considered as shown in Fig. 6. The crack tip radius in this computational model is about 0.1µm.

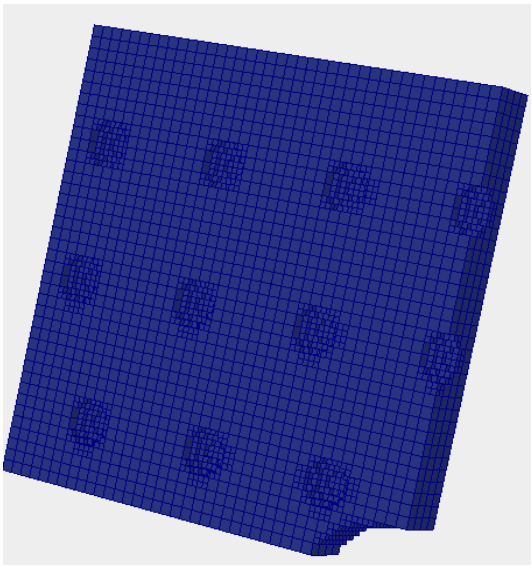

Figure 6: model of the precracked microstructure

Figure 7 illustrates the effect of the addition of particles with a radius of 50 nm on the fracture behavior of the compound. The same approach as in the previous section, based on the inelastic energy consumed up to the maximum stress, has been used. The results lead to the conclusion that the addition of particles to the matrix in such morphology and arrangement (Fig. 6) does not contribute to an enhancement in the dissipated energy at maximum stress in the model, which contradicts with experimental results.

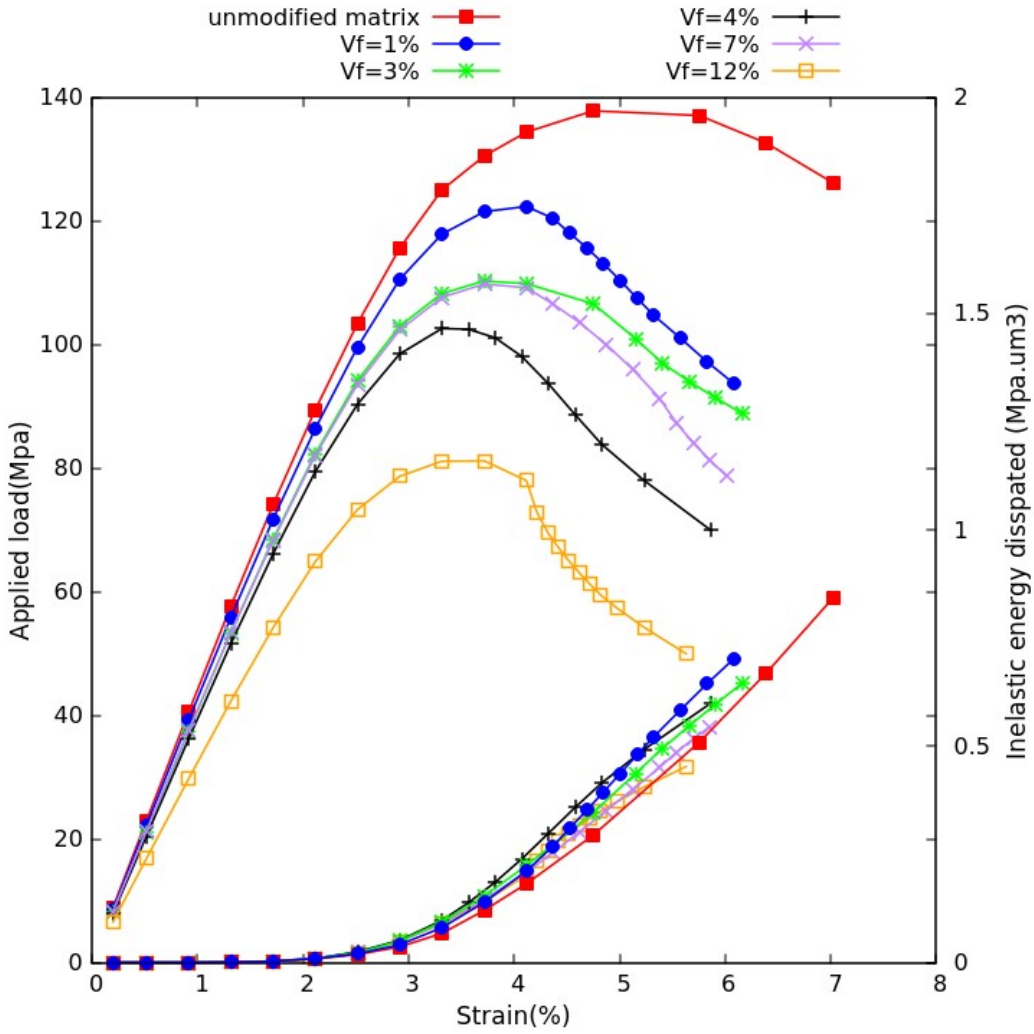

Figure 7: Effect of the particle concentration on the fracture toughness (Vf=volume fraction)

Being aware that the size and the arrangement of the particles can affect significantly the behavior of the compound, several attempts have been carried out in order to find an optimal morphology ensuring the enhancement of the dissipated energy at maximum stress. However, all attempts have led to a decrease in the dissipated energy compared to the unmodified matrix.

As an attempt to get more precise results, a further refinement of the mesh including 1% of particles with radius 50 nm has been performed by decreasing the element size by a factor of 0.5 (roughly

eight times as many elements). However, almost the same results have been found as can be seen in Fig. 8, in particular concerning the dissipated energy.

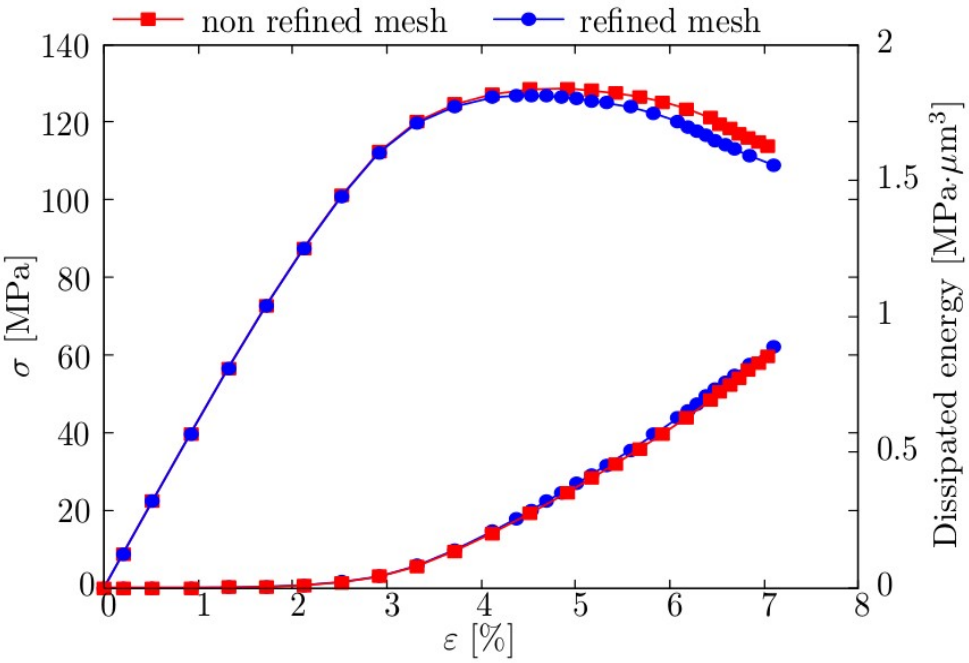

Figure 8: Mesh quality evaluation

As a conclusion, the model of the present work doesn't allow the prediction of the contribution of the particles dispersed around the precrack in Fig. 6 to the prevention of its propagation. This inefficiency could be the consequence of the fact that the fracture behavior is a multiscale problem while we consider only the microscale in the present study.

The assumption adopted that the void growth from cavitated rubber particles inside the particles is the dominant mechanism during the failure process of the material could also limit the efficiency of the present study. Indeed, other mechanisms involved during the loading of such materials, such as the cavitation, the crazing inside the particles or the interface debonding may lead to the absorption of more energy and then contribute to the prevention of the fracture progress in the matrix. Thus, more micromechanical studies are required to develop a more complete and efficient numerical model allowing a more precise prediction of the fracture toughness of core-shell nano-particle modified epoxies.

3.2. Application of the model to unidirectional carbon fiber-reinforced epoxy

3.2.1. Material properties calculation

A further project aim was the calculation of effective properties of carbon fiber-reinforced epoxy composites. To this end, a campaign of numerical tests, such as longitudinal and transversal tensile tests as well as in-plane shear tests, has been conducted. For this purpose, the unit cell (Fig. 2b) of

the composite, in a first step being assumed perfect without defects, has been used (defects will be considered in a later section). Figure 9 depicts the deformation resulting from each load case.

Table 5 shown below lists the predicted material properties as well as a confrontation of these calculated values to those measured by project partners. An acceptable agreement could be found with a slight gap that could be partially explained by the neglect of the defects being present in the real material.

Table 5: CFRP Material properties calculated vs. measured

	Calculated	*Measured*
Longitudinal Young's modulus	143480 (Mpa)	140000 (Mpa)
Transverse Young's modulus	6687 (Mpa)	7440 (Mpa)
In-plane shear Modulus	3640 (Mpa)	4720 (Mpa)
Transverse strength	97.9(Mpa)	83 (Mpa)
In-plane shear strength	---	73.58 (Mpa)
Longitudinal Poisson's ratio	0.28	0.31

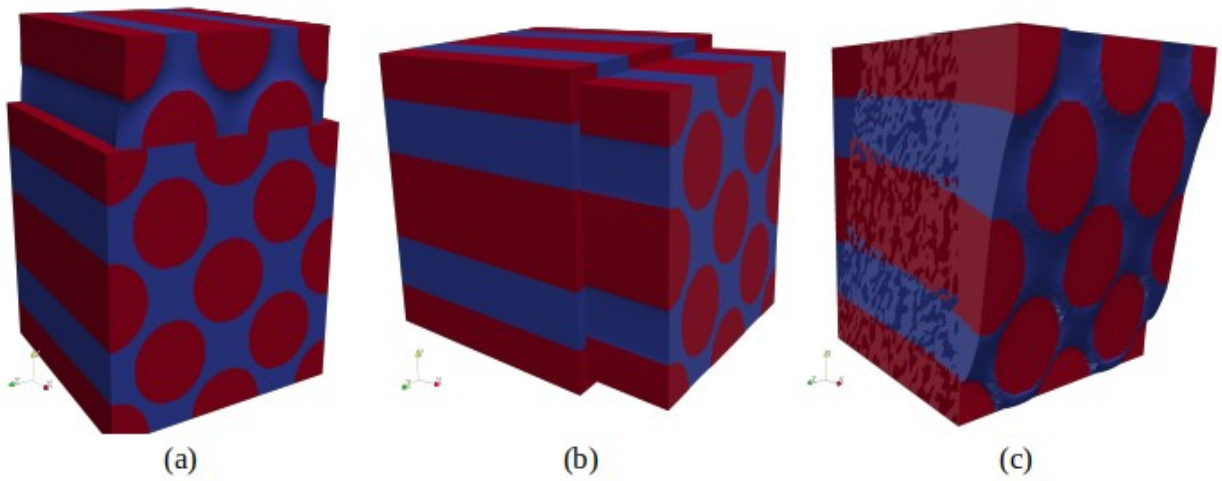

Figure 9: Composite unit cell under (a) transverse loading, (b) longitudinal loading, (c) in-plane shear loading

3.2.2. Fiber volume ratio effect

In this section, the CFRP-microstructure is varied based on an important parameter with a decisive effect on the performance of the composite which is the volume fraction of fiber reinforcement. Intuitively, a higher fiber volume fraction is usually expected to result in better mechanical properties of the composite.

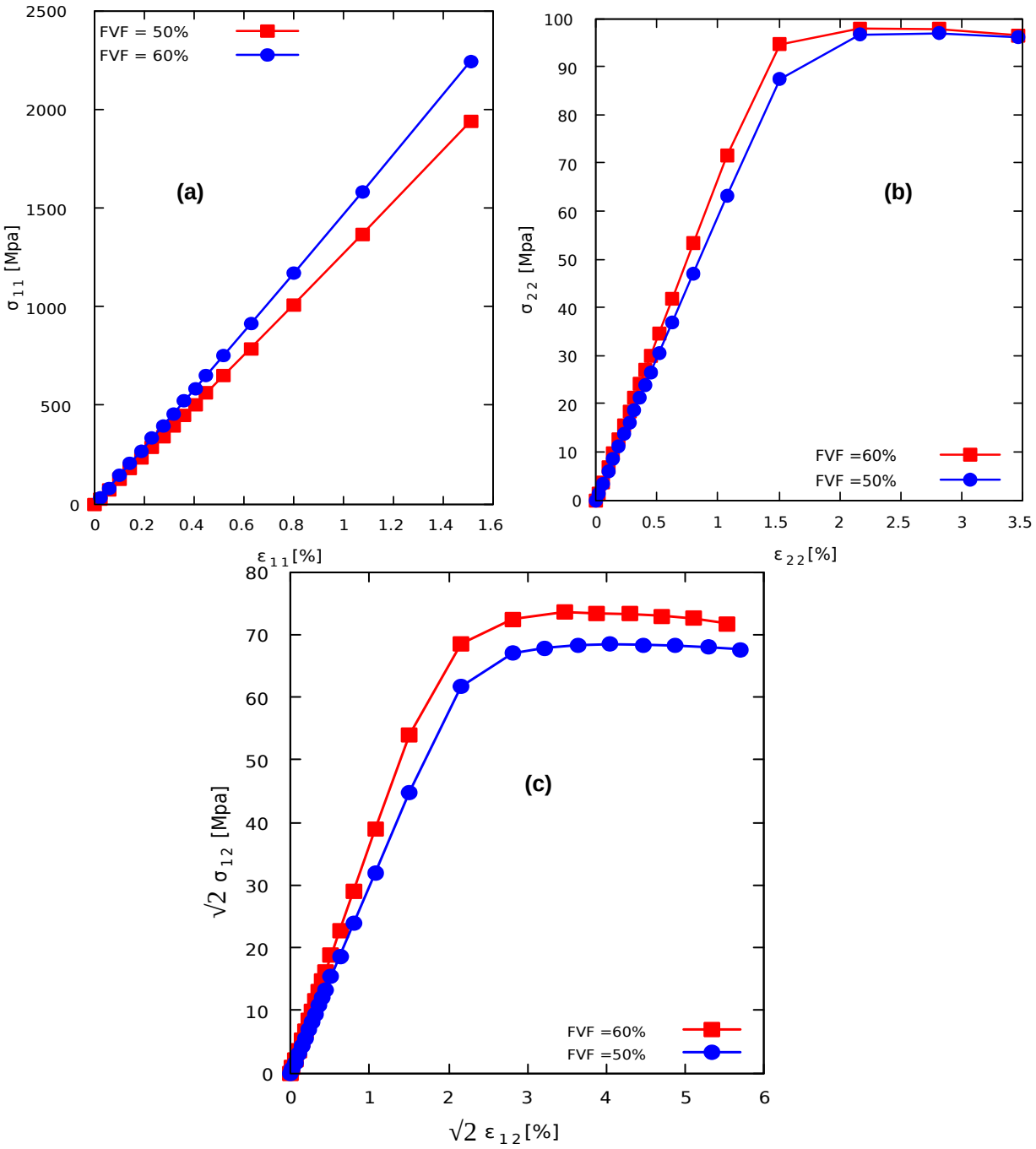

Figure 10: Fiber volume ratio effect on: (a) Longitudinal behavior, (b) Transverse behavior and (c) In-plane shear behavior

However, it has been demonstrated that an increase in fiber content does not always improve the energy-absorption capability of a CFRP material (Jacob, 2005). The accuracy of this observation has been assessed in the case of our material by the calculation of the energy absorbed up to the maximum stress level by the material subjected to transverse loading for two fiber fractions (50% and 60%). Thus, it was possible to build up a clear picture of the effect of this parameter on the overall behavior of the composite based on the results obtained through the conduction of a campaign of virtual experiments such as longitudinal and transverse tensile tests as well as in-plane shear tests. The results obtained from this investigation are presented below. It should be noted that in this investigation, the porosity has not been considered.

The mechanical behavior of the material being subjected to longitudinal and transverse tension as well as in-plane shear loading is illustrated in Fig. 10. At a first glance, one could assume that the more the fibers are included the better is the response of the material in terms of mechanical capacities.

However, it can be concluded from Table 6 that this is true only in terms of strength and stiffness, whereas the variation of the fiber fraction showed the already mentioned effect on the capability of the material to absorb energy. Indeed, the calculation of the energy up to the maximum stress according to each fraction for both transverse and in-plane shear loadings revealed that a CFRP with only 50 % of fibers absorbs more energy than the one with 60%.

Table 6: Fiber volume fraction (FVF) effect on mechanical properties of the composite

	FVF = 50%	*FVF = 60%*
E_{11} *(Mpa)*	126400	143480
E_{22} *(Mpa)*	5920	6687
G_{12} *(Mpa)*	2980	3630
σ_{22} *(Mpa)*	96,87	97,9
σ_{12} *(Mpa)*	68,43	73,58
ν_{12}	0,257	0,246
Absorbed energy (transv.) (Mpa)	1	0,63
Absorbed energy (shear) (Mpa)	0,75	0,64

Therefore we can confirm through our numerical study it is not always true, that an increase in the fiber content necessarily improves the energy absorption capability indicative of the composite material toughness.

A possible explanation for this finding is that as the fiber volume fraction increases, the volume of the matrix between the fibers decreases. This causes an increase of strain localization in the matrix, leading to matrix cracks forming at lower loads, which results in an early failure and a reduction in the amount of the energy absorbed before the maximum stress.

This assertion could be backed up by Fig. 11, which shows the damage distribution throughout the unit cell at an early level of transverse loading for both volume fractions of fibers 50% (diameter of fibers = 6,5µm) and 60% (diameter of fibers = 7µm). From this figure, one can notice that at the same level of loading (low) the material with higher fiber volume fraction exhibits a more pronounced intensity of damage in the matrix .

This high intensity of damage reflects the early creation of matrix cracks being at the origin of the low toughness (or also called energy absorption capability) found for this material combination.

A look into Table 6. confirms that in order to identify an optimized composite material based on the fiber fraction parameter we must seek a compromise. The decision definitely depends on the required application-specific performance and a thought must be also given to the cost which can be reduced by the manufacturing of the rotor cap with less carbon fibers while ensuring a better toughness.

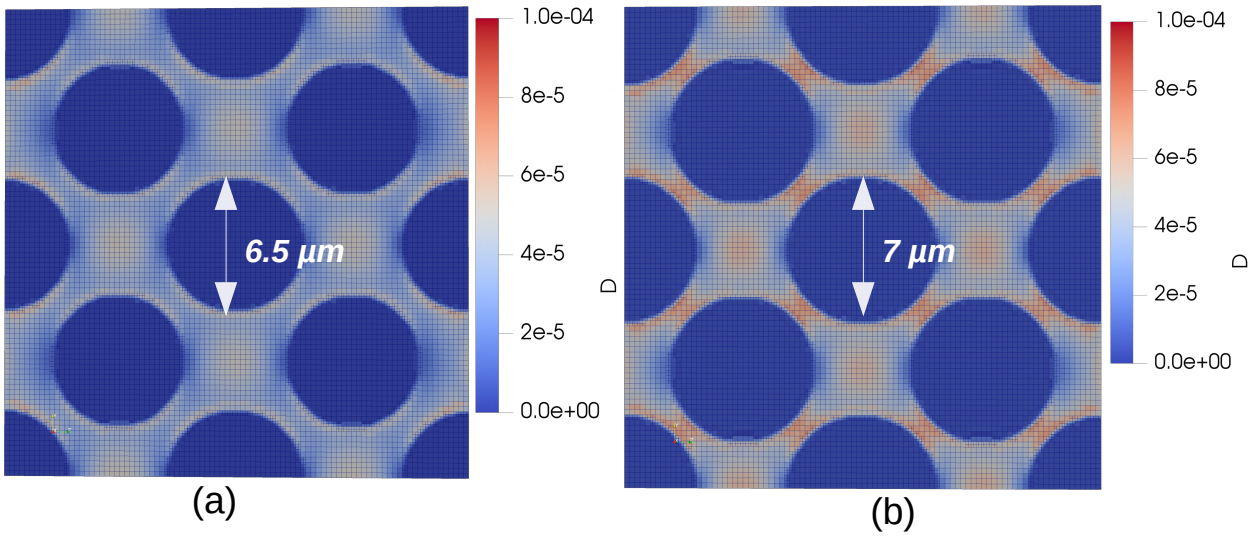

Figure 11: Fiber fraction effect: damage distribution in the composite unit cell under low transverse loading for (a) FVF = 50 % and (b) FVF = 60%

3.2.3. Fiber shape effect

In order to acquire a more complete picture about the effect of the microstructure variability on the overall behavior of the composite another parameter has been taken into account in our study which is the shape of the fibers. In addition to typical fibers with circular cross sections, another type of

fibers with non-circular cross sections (or also called elliptical fibers), being available on the market, has been considered.

The unit cell of such a combination is shown in Fig. 12 Here, voids are not modeled and a typical volume fraction of fibers of 60% is considered.

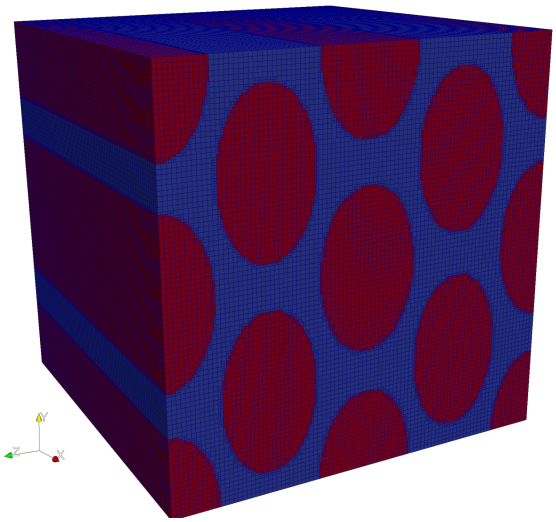

Figure 12: Unit Cell of the composite reinforced by 60% of elliptical fibers

A comparison between the responses obtained from the conduction of longitudinal, transverse and in-plane shear loadings on two different unit cells of composites reinforced by 60% of elliptical and circular fibers, respectively, is illustrated in Fig. 13. The figure shows that the alteration from circular to elliptical fibers has a mild enhancement effect on the longitudinal and the transverse behavior of the overall material. However, a significant enhancement in terms of in-plane shear properties could be granted to this alteration.

The enhancement caused by the introduction of elliptical fibers instead of circular fibers does not only cover the stiffness and the strength but also the energy absorption capability. Indeed, the energy absorbed by the material up to the maximum transverse stress is enhanced by 11% versus a 61% of enhancement in the case of in-plane shear loading.

This result could be supported by the study of Yoon et al. (1997) who found out that elliptical-shaped cross-sections of the carbon fibers lead to a lower tendency to form transverse cracks, compared to circular cross-section carbon fibers, which makes the material maintain its transverse strength and its energy absorption capacity or toughness.

Table 7 collects the values of all parameters calculated through this investigation. The analysis of this table leads to favor elliptical fibers over cylindrical fibers but the compromise with the possibility and the cost of such fibers should be taken into account.

To accomplish a complete study about the effect of the fibers' shape on the material properties, several other shapes applied in industry, such as Y-shape and C-shape (Park et al., 2004), could in principle be considered, which was not possible because of the tight timeline of the project.

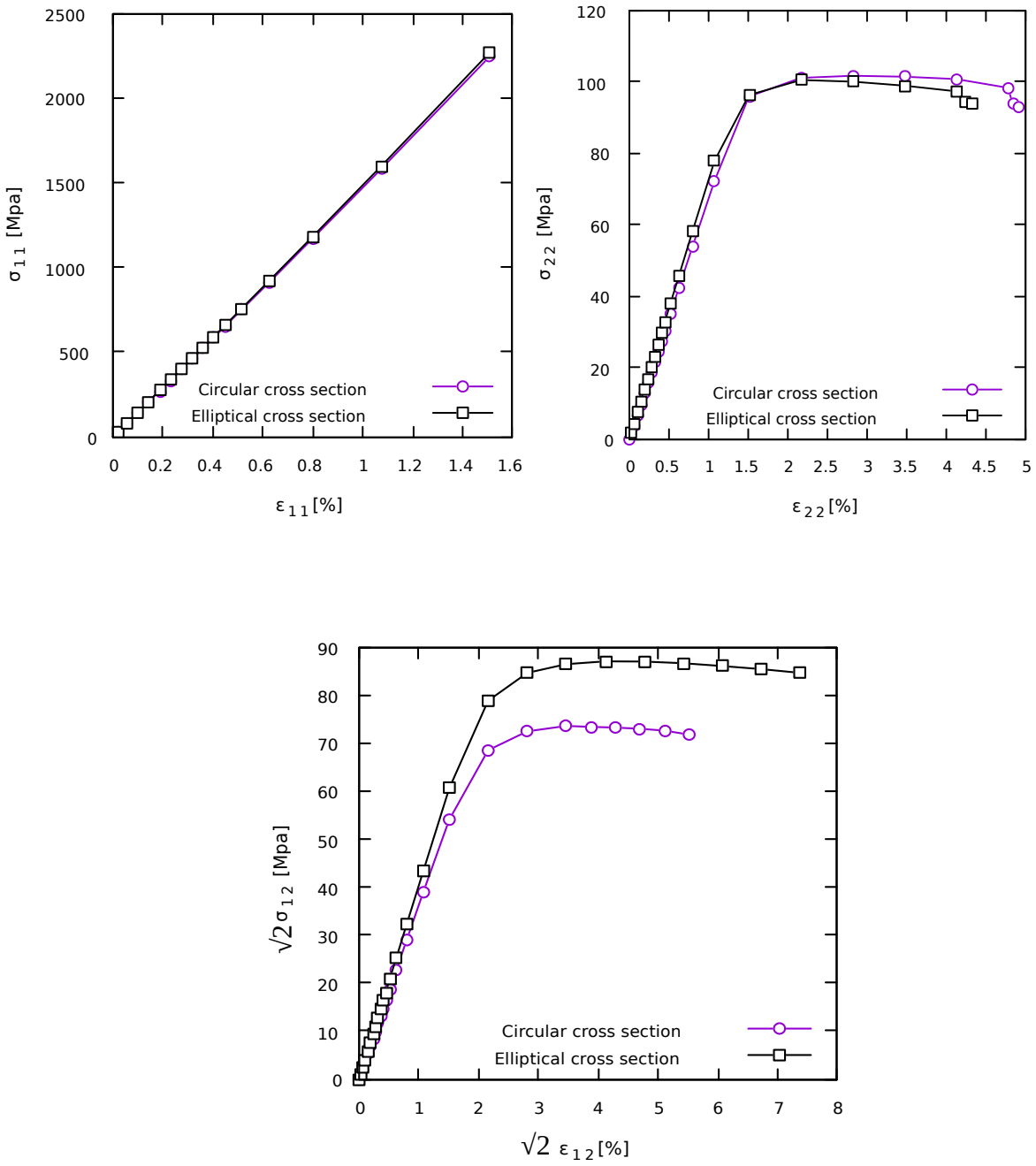

Figure 13: Fiber shape effect on: (a) Longitudinal behavior , (b) Transverse behavior and (c) In-plane shear behavior

Table 7: Fiber shape effect on mechanical properties of the composite

	Elliptical fibers	Circular fibers
E_{11} *(Mpa)*	145400	143480
E_{22} *(Mpa)*	7300	6687
G_{12} *(Mpa)*	4049	3630
$\sigma_{22,max}$ *(Mpa)*	100,4	97,9
$\sigma_{12,max}$ *(Mpa)*	87	73,58
ν_{12}	0,2544	0,246
Absorbed energy (transv.) (Mpa)	0,7	0,63
Absorbed energy (shear) (Mpa)	1,03	0,64

3.2.4. Matrix voids effect

The intensive investigation of the formation and the characteristics of voids present by default in fiber-reinforced polymer composites is motivated by the awareness of the relevant effect of such manufacturing defects on the mechanical performance, which are therefore also investigated in this project.

The experimental work carried out in this field during the last five decades contributed to a large database enabling the assimilation of the formation of the voids as well as the estimation of their effects on the thermomechanical behavior of the composite. However, most of the studies in this context correlate the degradation of mechanical properties with the void content and don’t take into account other void-related parameters such as size, shape and spatial distribution.

Mehdikhani et al. (2019) listed in their review article related studies that emphasized the relevant effects of parameters other than the voids’ amount on the mechanical performance of fiber-reinforced composites. Therefore to draw accurate conclusions in regard to the effects of voids, an investigation based on the variation of different parameters is required.

Studies based on modern characterization techniques such as FE numerical modeling are as well multiplying and more and more are boosted by the industry to deal with this relevant issue. This represents one of the main focuses of this project aiming for an optimized manufacturing process resulting in an effective composite material. In this section, results obtained through the investigation of the voids’ effect on the transverse behavior of the carbon fiber-reinforced epoxy for the rotor cap will be presented and analyzed.

The fiber fraction considered in this part of the study is again 60%, however in order to simplify the problem and to save time, the unit cell considered here is not a cube but exhibits a thin thickness, as the incorporation of voids requires a higher mesh refinement, leading to longer simulation times.

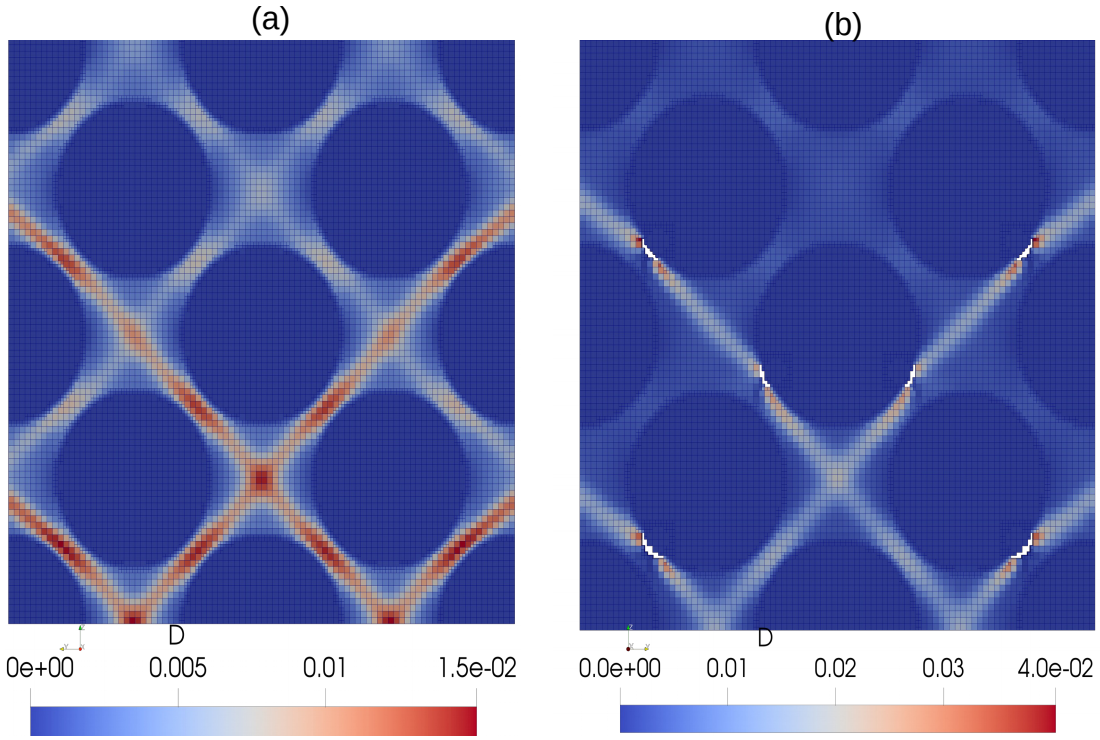

Figure 14: Damage distribution at the same load level in the CFRP (a) without voids and (b) with voids

The voids being modeled in this study represent matrix defects whose considerable effect can only be noticed in the transverse (not longitudinal) behavior. Therefore only a transverse tensile test has been simulated to carry out this investigation.

Prior to the variation of the voids' parameters and the assessment of the effect of this variation on the material properties, we illustrate in Fig. 14 a general overview of the effect of such defects on the failure behavior of the material. The figure shows the distribution of damage in the material without and with voids. Obviously, the presence of the voids, even with a small volume fraction of 0,2%, affects the damage formation and distribution throughout the material. In particular the maximum damage is increased compared to the situation without voids and the damage localizes in the vicinity of the voids, as one would expect.

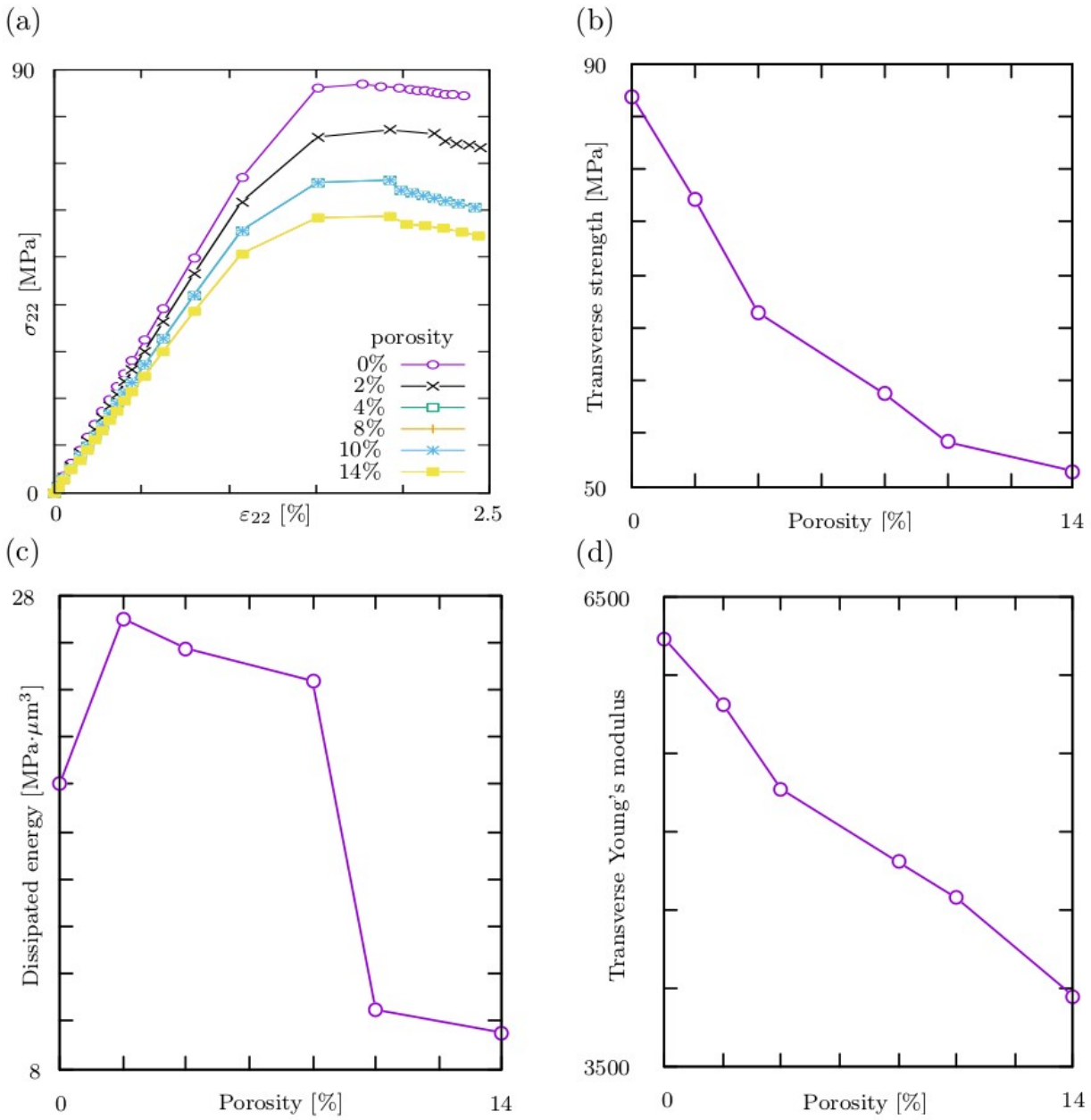

Figure 15: Effect of the porosity: (a) Transverse responses , (b) transverse strengths, (c) dissipated energy of the material with different void volume fractions, (d) transverse modulus

3.2.4.1. Porosity effect

To investigate the effect of the porosity amount, five void volume fractions have been considered in addition: 2%, 4%, 8%, 10% and 14%. Results obtained from this investigation are presented in Fig. 15.

As expected, the incorporation of voids into the CFRP material causes a dramatic decline in the transverse strength and stiffness. For instance, 4% of void content causes a reduction of 25% for the strength $\sigma_{22,max}$ and 18% for the transversal Young's modulus E_{22}. However, the result in Fig. 15c

was not necessarily expected. Indeed, the energy absorption capability of the material is improved up to 8% of voids content compared to the defect-free material. This observation is confirmed by several experimental studies with similar material systems (Mehdikhani et al, 2019). The physical explanation suggested for this unexpected finding is that around these voids new plastic zones are formed allowing for extra energy-absorption. Though, it should be noted that this enhancement is granted to a specific reduced fraction of porosity which is estimated according to our investigation up to 8% porosity.

Based on these findings, one could assume that a manufacturing process leading to a matrix porosity fraction up to 8% in the carbon fiber-reinforced epoxy could be approved, if the enhancement in the energy absorption capability is required and the sacrifice in terms of transverse stiffness and strength is acceptable.

3.2.4.2. Void distribution effect

To investigate the effect of the void distribution on the transverse behavior of the material, 2% of void volume fraction has been considered. This amount of porosity has been represented by 4 voids of diameter equal to 1,5 µm. Figure 16 (right) shows two kinds of void arrangement. In the first one, the 2% of porosity are represented by a void cluster and in the other one, the voids are well distributed.

The numerical investigation shows that the accumulation of voids results in a slight gain in terms of transverse stiffness and transverse strength (respectively +3,6% and +1,3%) against a significant loss in terms of deformation and energy absorption capability (-21% and -66%, respectively). Corresponding calculated values are shown in Table 8. It can be concluded that the material with well-distributed pores deforms more and absorbs more energy before reaching the maximum stress, which occurs earlier when defects are accumulated. This observation illustrates the deleterious effect of accumulated manufacturing defects on the CFRP material properties.

Table 8: Defect arrangement effect on transverse properties of the CFRP composite

	Pores diameter = 1µm *Porosity =2%* *well-distributed*	*Pores diameter = 1µm* *Porosity =2%* *accumulated*
E_{22} *(Mpa)*	5812	6041
$\sigma_{22,max}$ *(Mpa)*	77,1	78,1
ε_{22} *at* $\sigma_{22,max}$	1,91	1,5
Absorbed energy $_{22}$ (Mpa.µm^3)	26,97	9,18

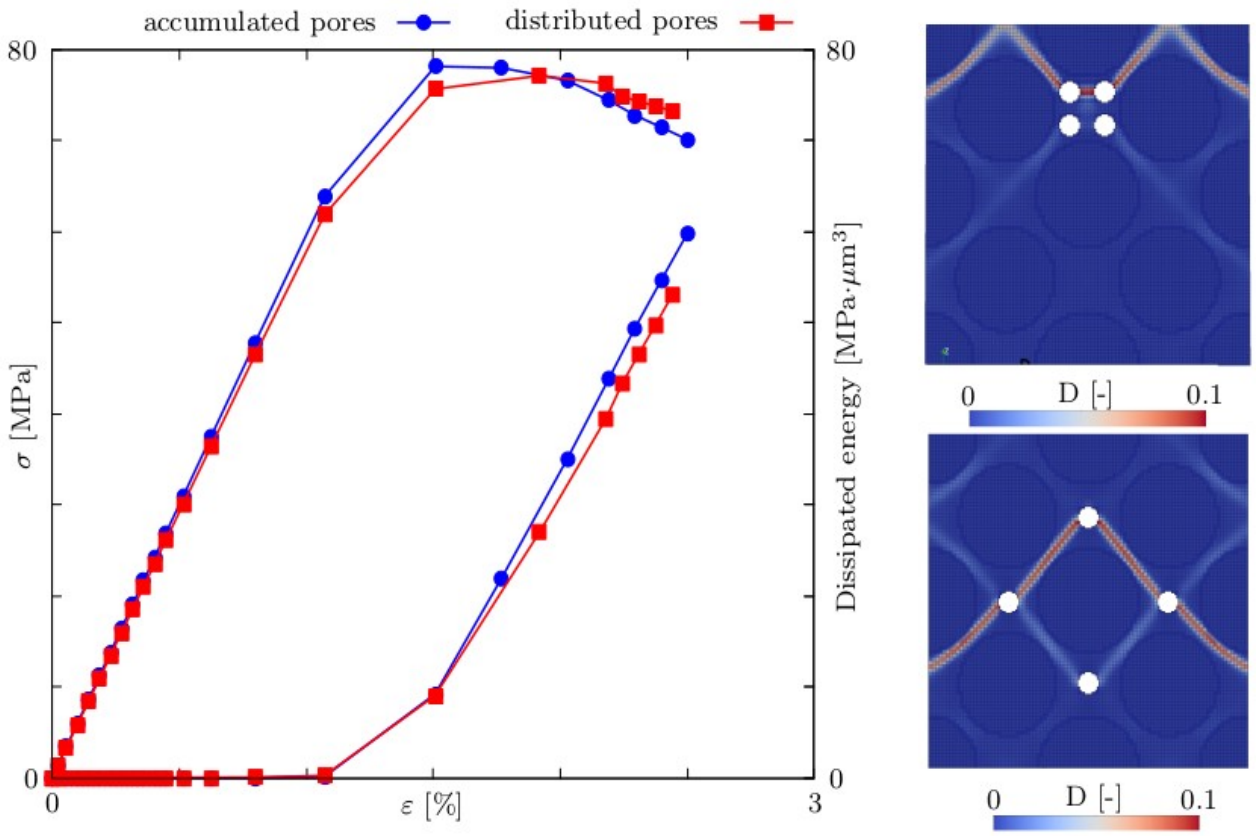

Figure 16: Void distribution effect on the transverse behavior of the CFRP material

3.2.4.3. Void size effect

According to Fig. 17, the decrease of the diameter of the voids from 1,5 µm to 1 µm, while maintaining the same volume fraction (2%), has a slightly negative effect on the transverse behavior of the overall composite. The maximum stress and the strain at that stress have decreased, respectively, by 2% and 4% which led to a decrease in terms of energy absorption of 13%. These effects are small, and may also be influenced by the slightly different void distribution in both cases. Concerning the stiffness, a negligible effect with a decrease of 0,7% has been seen. Table 9 collects all the transverse properties calculated for void pore sizes.

Table 9: Void size effect on transverse properties of the CFRP composite

	Void diameter = 1.5µm *Porosity =2%*	*Void diameter = 1µm* *Porosity =2%*
E_{22} *(Mpa)*	5812	5778
σ_{22} *(Mpa)*	77,1	75,35
ε_{22}	1,91	1,83
Absorbed energy (Mpa.µm^3)	26,97	23,3

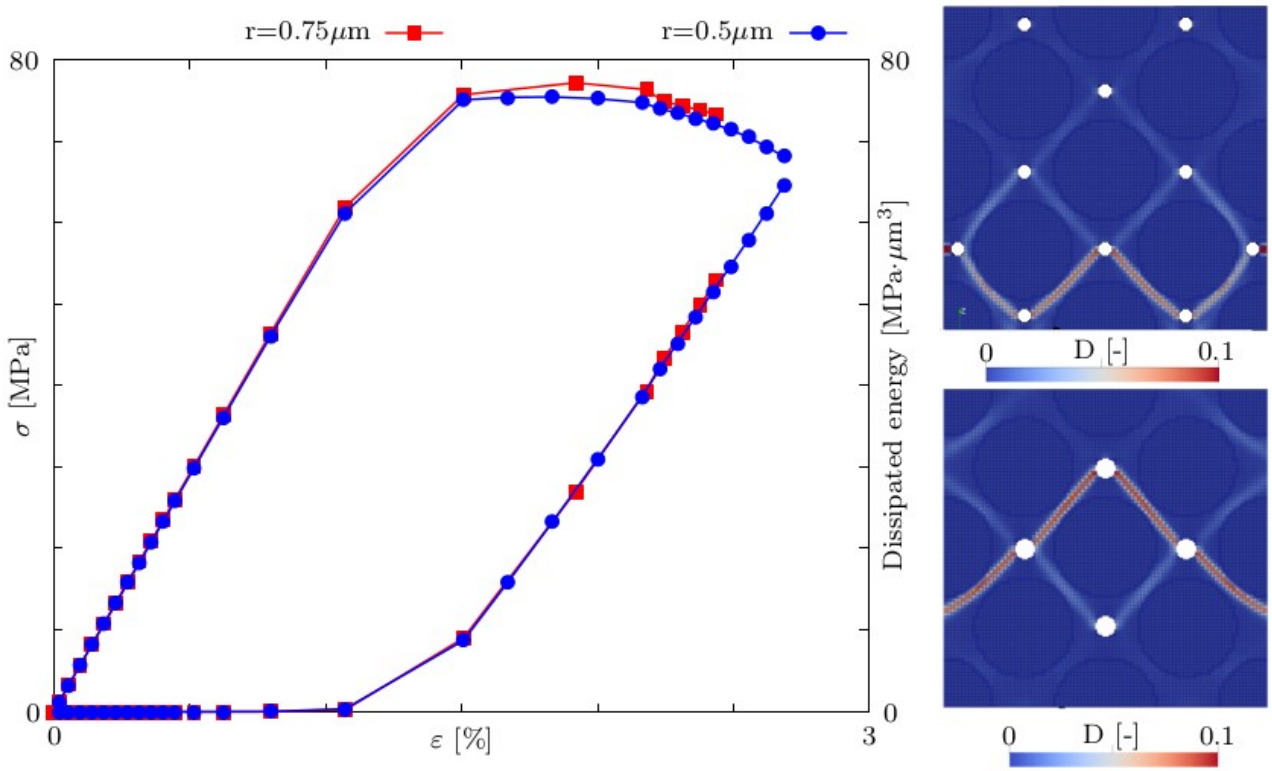

Figure 17: Void size effect on the transverse behavior of the CFRP material

3.3. Application of the model to woven glass fiber-reinforced epoxy

One of the project goals involved the improvement of the understanding of failure mechanisms governing the degradation of the insulation system of the turbo generator, which includes as a core component a composite made of woven glass-fibers, being embedded in an epoxy-matrix. For this purpose, the model in Fig. 2c has been applied (see also the explanatory text in Sect. 2.3).

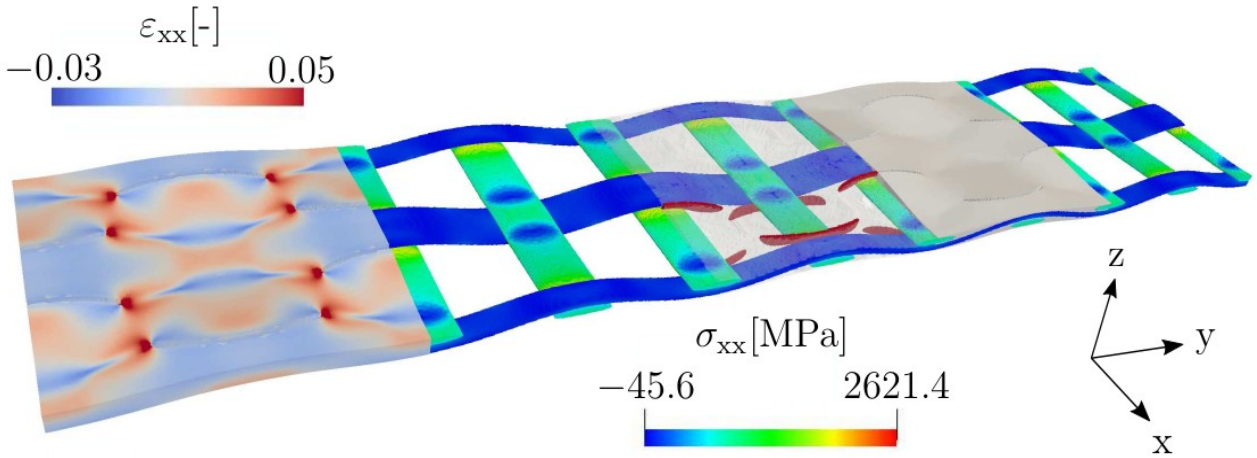

Figure 18: Simulation of woven roving model with monitoring of strains, stresses and cracks. The cracks are visible on the (white) surface, while internal cracks are visualized in red color (center of the figure).

The monitoring of strains and stresses in the rovings and cracks in the matrix over the course of the simulation are visualized in Fig. 18. At the intersection of the rovings the maximum stresses and the initiation of cracks in the matrix can be observed (marked in red in the center of the figure). The maximum strains are found at the tips of the growing cracks (Fig. 18, left).

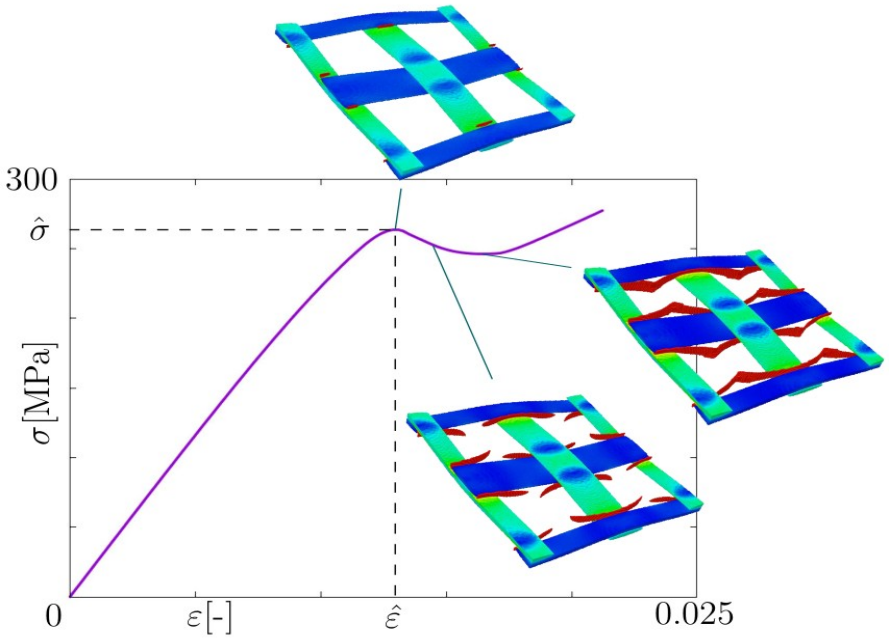

Figure 19: Stress strain response of woven roving composite and growth of internal cracks (in red color)

Only when the cracks fully traverse the sample, the stress increases again, since then the rovings start to straighten. For an improved resistance to cracking it is therefore interesting to find material and geometry parameters that increase $\hat{\sigma}$ and $\hat{\varepsilon}$.

The predicted influence of vertical roving thickness on Young's modulus *E* and crack initiation stress $\hat{\sigma}$ and strain $\hat{\varepsilon}$ is illustrated in Fig. 20. The dimensions (in mm) of the thinnest structure, depicted in Fig. 20, are 1mm×1mm×0.0625mm and the major and minor half axes of the rovings' elliptic cross section are 0.2mm and 0.0125mm, respectively. The results indicate an advantage of vertically thinner rovings of the compound material.

Next, the influence of the lateral roving thickness on $\hat{\sigma}$ and $\hat{\varepsilon}$ was investigated. Here, the thicker structure (thickness ratio 1) is identical to the thinnest one from the vertical thickness comparison (Fig. 20). However, the matrix is slightly softer (E_M = 3039 MPa) in order to investigate also the stiffness' influence. The results (see Fig. 21) show for a thickness increase by a factor of 2 an increase in $\hat{\sigma}$ in the order of 100MPa but a decrease in $\hat{\varepsilon}$ by almost one third. Thus, depending on the case, either a higher or a lower lateral thickness might be the better choice. However, as the product of $\hat{\sigma}$ and $\hat{\varepsilon}$ and thus the energy necessary for cracking slightly increases for laterally thicker rovings, in general a higher lateral thickness might be advantageous, although the effect is not as pronounced as for the vertical thickness.

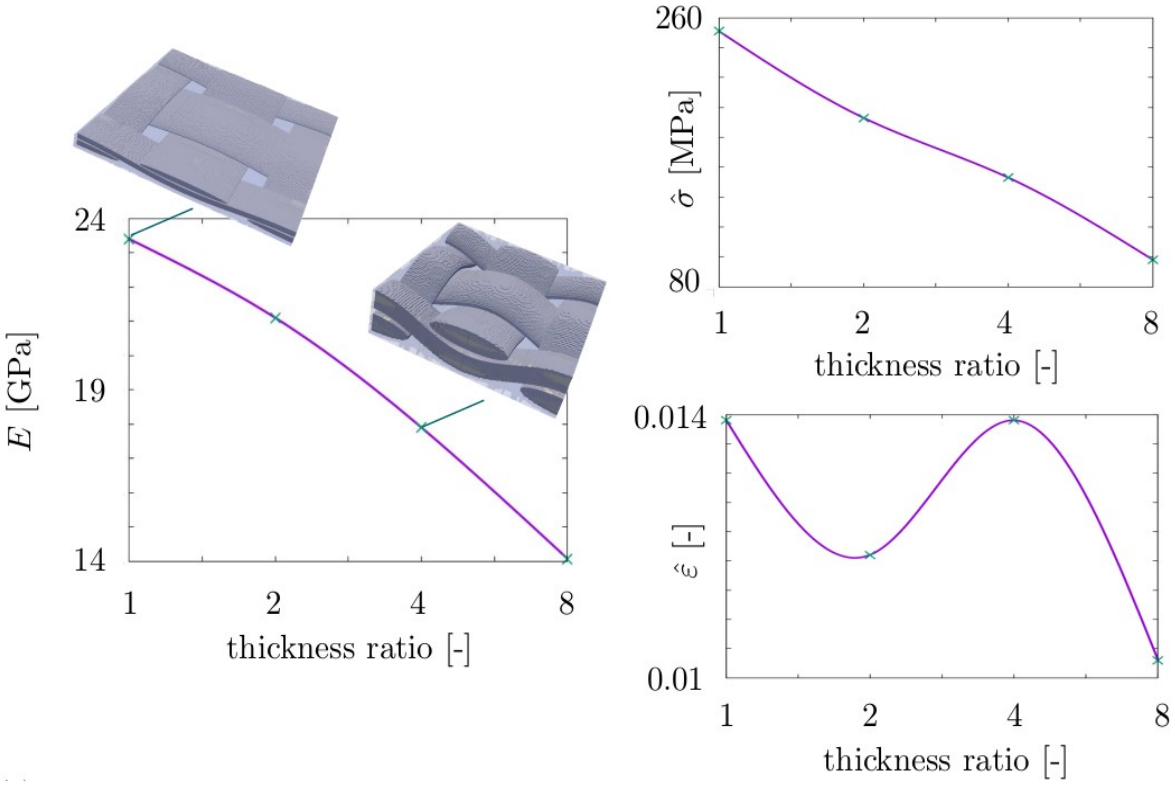

Figure 20: Influence of vertical roving thickness on Young's modulus E and crack initiation stress $\hat{\sigma}$ and strain $\hat{\varepsilon}$

Finally, the influence of Young's modulus E_{roving} of the rovings and the elastic energy release rate g_c^e of the matrix material on the overall crack resistance was investigated. The results are depicted in Fig. 22. A higher value of Young's modulus of the rovings leads to an increase in $\hat{\sigma}$ and a decrease in $\hat{\varepsilon}$. In case of an increased matrix elastic energy release rate, both $\hat{\sigma}$ and $\hat{\varepsilon}$ are also increased.

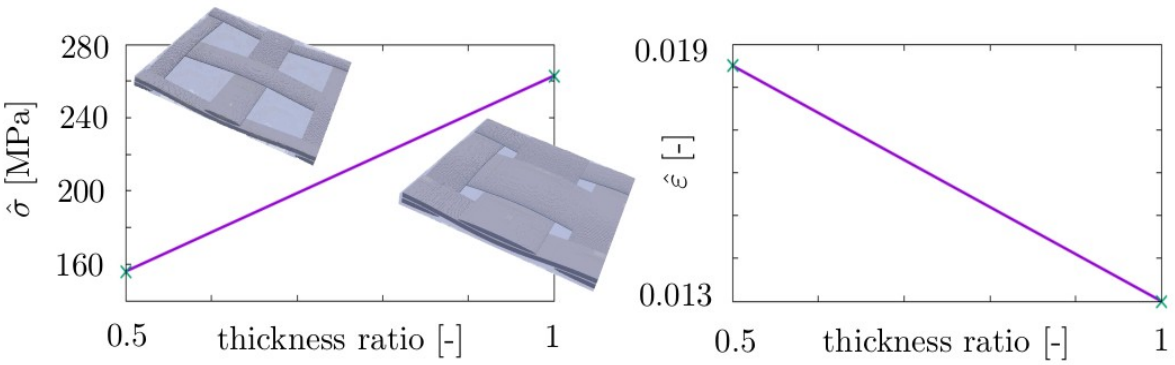

Figure 21: influence of lateral roving thickness on $\hat{\sigma}$ and $\hat{\varepsilon}$

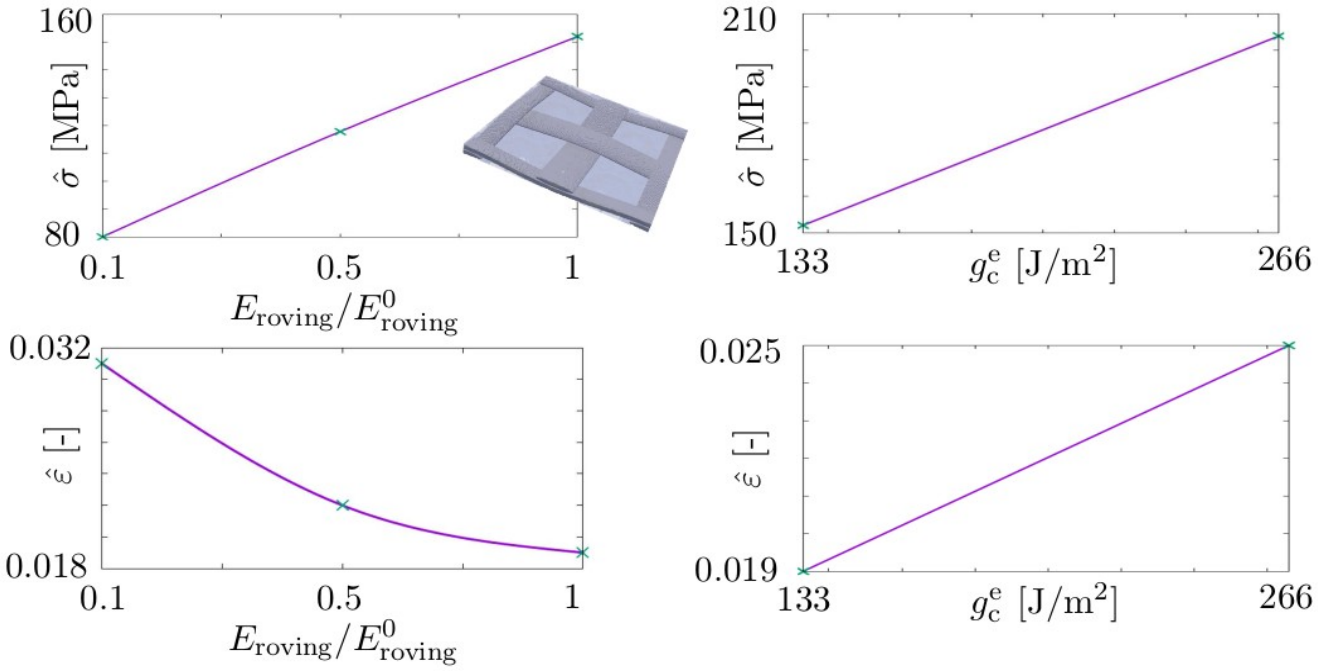

Figure 22: Influence of Young's modulus of roving material and elastic energy release rate of matrix material on crack initiation stress $\hat{\sigma}$ and strain $\hat{\varepsilon}$ with E_{roving} = 47.49GPa and ν_{roving} = 0.25

3.4. Thermal study

Besides the estimation of mechanical properties, the computer-aided estimation of thermal effective conductivities for the different composite microstructures was a further goal of the project. Materials with low thermal conductivity can't well divert the heat accumulated which could lead to the degradation of their mechanical properties particularly if the functioning of the product involves high temperature as is the case in the turbo generator considered in this project. Epoxy is a thermoplastic resin, which is a good thermal insulator with a thermal conductivity arount 0,2 W/Km. This key property is typically increased by the inclusion of fillers with a higher capability to conduct heat. Obviously, the configuration and the amount of the composite constituents affect the heat dispersion in the composite and thus its overall thermal conductivity. This effect has been investigated in the specific cases of the materials (considered in the previous sections) of the project and the results obtained are presented and discussed in the following sections.

Unit cells considered to perform the thermal characterization of each composite are in analogy to the ones used in the mechanical characterization. Here, the thermal loading is given in terms of an imposed macroscopic temperature gradient in a given direction. Moreover, the fluctuation of the temperature is considered null at all boundaries, for simplicity.

To calculate the thermal conductivities of the composites with specific microstructures, the heat flux vector q is computed by means of the heat conduction equation or also called the Fourier's law

$$q = -k \text{ grad } (T),$$

where *k* is the thermal conductivity whose general form is a second-order tensor for anisotropic materials and a scalar for isotropic materials. The thermal properties of the constituents of the composits will be assumed isotropic, for simplicity, while the effective behavior, which is to be simulated, is anisotropic. That is, the major aim is to compute the aforementioned second-order tensor for the different composites.

Thermal conductivities of each component of the three composites considered in these thermal investigations (found in the literature) are presented in Table 10.

Table 10: Thermal conductivities of composite componenents

	Epoxy	Carbon fibers	Glass fibers	Rubber
Thermal conductivity [W/Km]	0,2	6,9	0,05	0,29

3.4.1. Core-shell-rubber particle modified epoxy

As shown in Table 1, the thermal conductivity of the rubber is very close to the one of epoxy, so it is expected that the enhancement of the overall thermal conductivity will be minor. As will be exemplarily shown, the thermal behavior of this material is such that the heat flux depends isotropically on the gradient of the temperature, as expected. Therefore, only one thermal conductivity will be characterized for each CSRP-microstructure.

3.4.1.1. Effect of the particle volume fraction and size

To investigate the effect of the size and of the volume fraction of the particles on the thermal conductivity of the overall composite, particles with two different radii R_{part}=25nm and R_{part}=50nm and different volume fractions ranging between 0% and 15% have been considered. A typical unit cell is shown in Fig. 24b.

Figure 23 illustrates a comparison between thermal conductivities obtained for each particle size with different volume fractions. It could be easly noticed from this figure that the more particles are included in the unit cell, the more the thermal conductivity is enhanced and that the same values are obtained for both sizes of particles when are they included with the same amount.

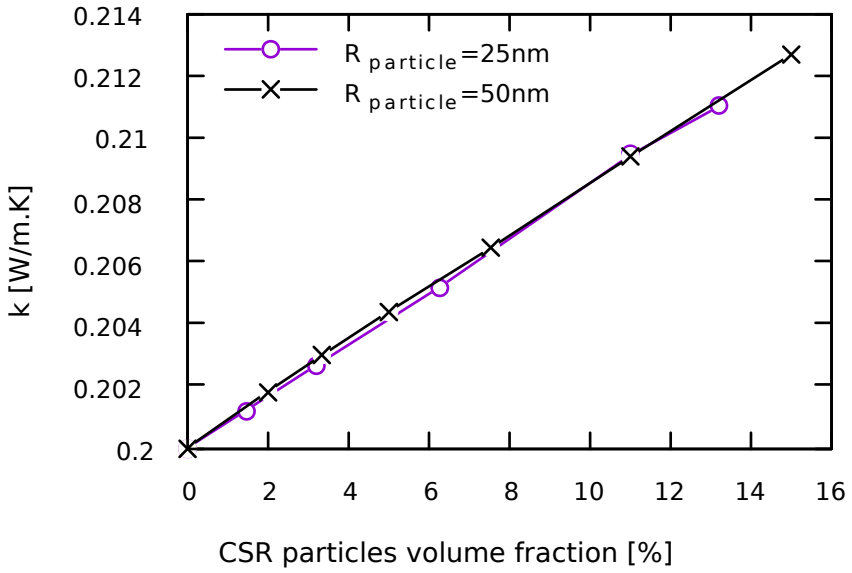

Figure 23: Effect of the particle size and the volume fraction on the thermal conductivity of the CSR/epoxy composite

3.4.1.2. Effect of the particle distribution

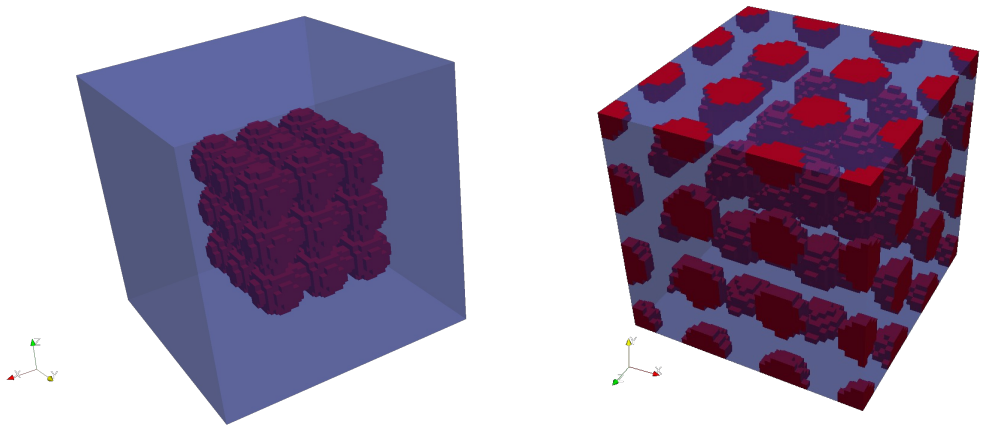

Figure 24: unit cell of the CSR/epoxy composite with (a) clustred particles, (b) well distributed particles

To find out whether the distribution of the particles has an effect on the propagation of the heat through the unit cell, two unit cells with two different distributions have been considered. Figure 24a shows a unit cell including 11% of particles with a radius of 50nm, which are accumulated in a cluster.

The same amount and size characterize the particle distribution in the unit cell shown in Fig. 24b. However, a homogeneous dispersion has been considered in order to investigate the effect of the distribution. The heat fluxes related to each configuration has been calculated by three simulations

each, with prescribed macroscopic temperature gradients in all three spatial directions and the results obtained are shown in Table 11.

Table 11: Heat fluxes of CSR/epoxy composite

	Particles well distributed	Particles clustred
q1	(-0.20939, -0.49604E-18, 0.46614E-18)	(-0.20968 , 0.28704E-04, 0.28704E-04)
q2	(-0.43062E-18, -0.20939, -0.13431E-18)	(0.28704E-04, -0.20968, 0.28704E-04)
q3	(0.44931E-18, -0.13974E-18 , -0.20939)	(0.28704E-04, 0.28704E-04, -0.20968)

It can be observed from the values presented in Table 11 that the component of the heat flux related to the direction of the thermal loading (gradient of temperature) is almost the same for both configurations. The thermal behavior remains isotropic even with clustered particles.

Figure 25 illustrates the propagation of the heat flux and temperature fluctuations through the unit cell of the composite. The fluctuations of the temperature in the matrix are more pronounced at the level of the particles.

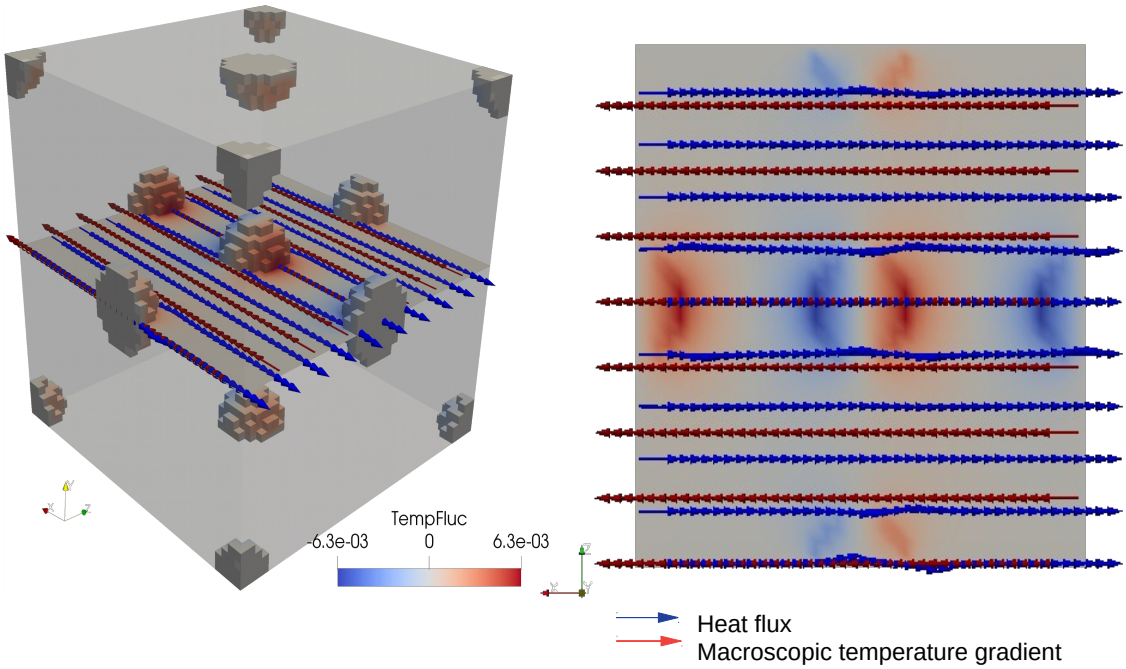

Figure 25: Distribution of the heat flux throughout the CSR/Epoxy composite: thermal fluctuations (in °C) and heat flux distribution

3.4.2. Carbon-fiber-reinforced epoxy

Figure 26 illustrates the heat flux through the unit cell of the CFR/epoxy composite. The arrows represent the heat flux, which is more important in the fibers. This was expected, as the thermal conductivity of the fibers is three times more important than the one of the epoxy matrix.

The simulation of the response of the unidirectionnal CFR/epoxy composite exposed to a macroscopic temperature gradient established the anisotropy of its thermal behavior. Indeed, it was demonstrated that the capability of this composite to conduct heat is more important in the direction of the fibers (eigenvalues $k_1 > k_2$ and k_3 of the heat conductivity tensor). Therefore, to investigate the effect of the microstructural configuration of the composite on the overall thermal behavior, the fully anisotropic heat conductivity tensor has been computed for each microstructure considered.

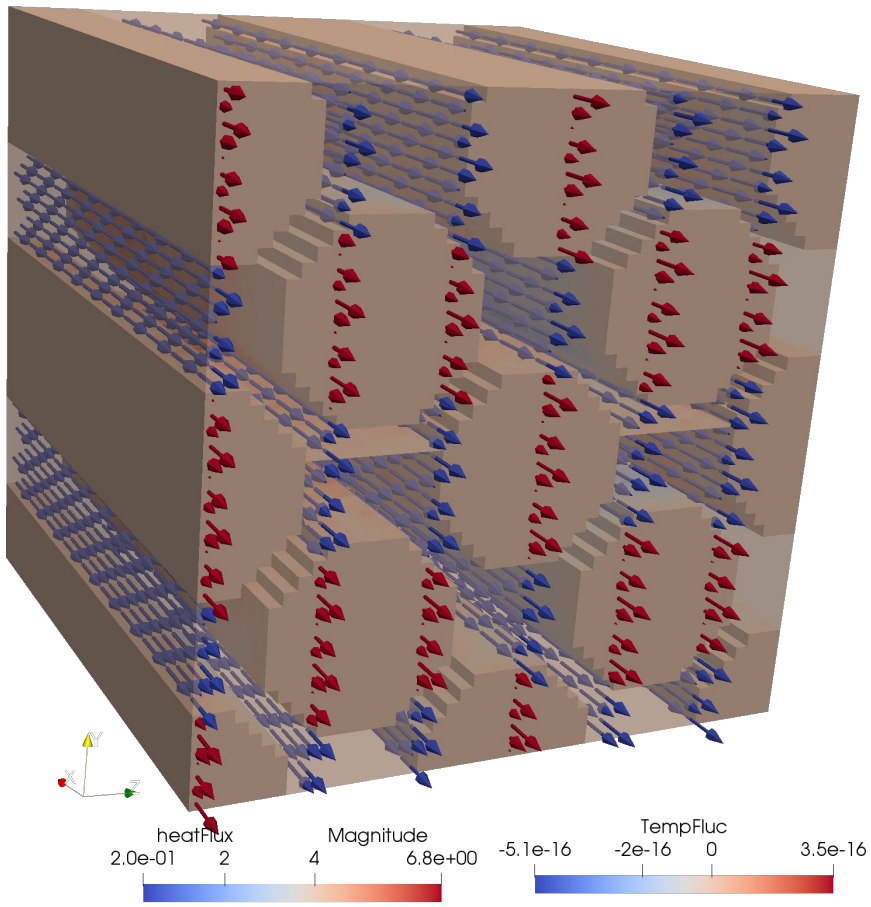

Figure 26: Distribution of the heat flux through the CFR/epoxy composite (heat flux in W/(m²s), temperature fluctuation in °C)

3.4.2.1. Fiber diameter and volume fraction effect

To investigate the size and volume fraction effect on the thermal conductivity of the overall CFR/epoxy composite three radii (R_f=3µm, R_f=3.5µm, R_f=4µm) and three volume fractions (V_f≈38%, V_f≈58% and V_f≈72%) have been considered when modeling the carbon fibers of this composite.

Figure 27 highlights the effect of the size and the volume fraction of the carbon fibers reinforcing the composite involved in the manufacturing of the rotor cap. Given that the thermal conductivity of the carbon fibers is greater than that of the epoxy resin, it was expected that the thermal conductivity of the overall reinforced composite would increase. And this enhancement is more pronounced with more carbon fibers added. This observation is well illustrated in Fig. 27. The figure shows also that the radius of the fibers has no effect on the thermal conductivity in the direction of the fibers when the same volume fraction is considered.

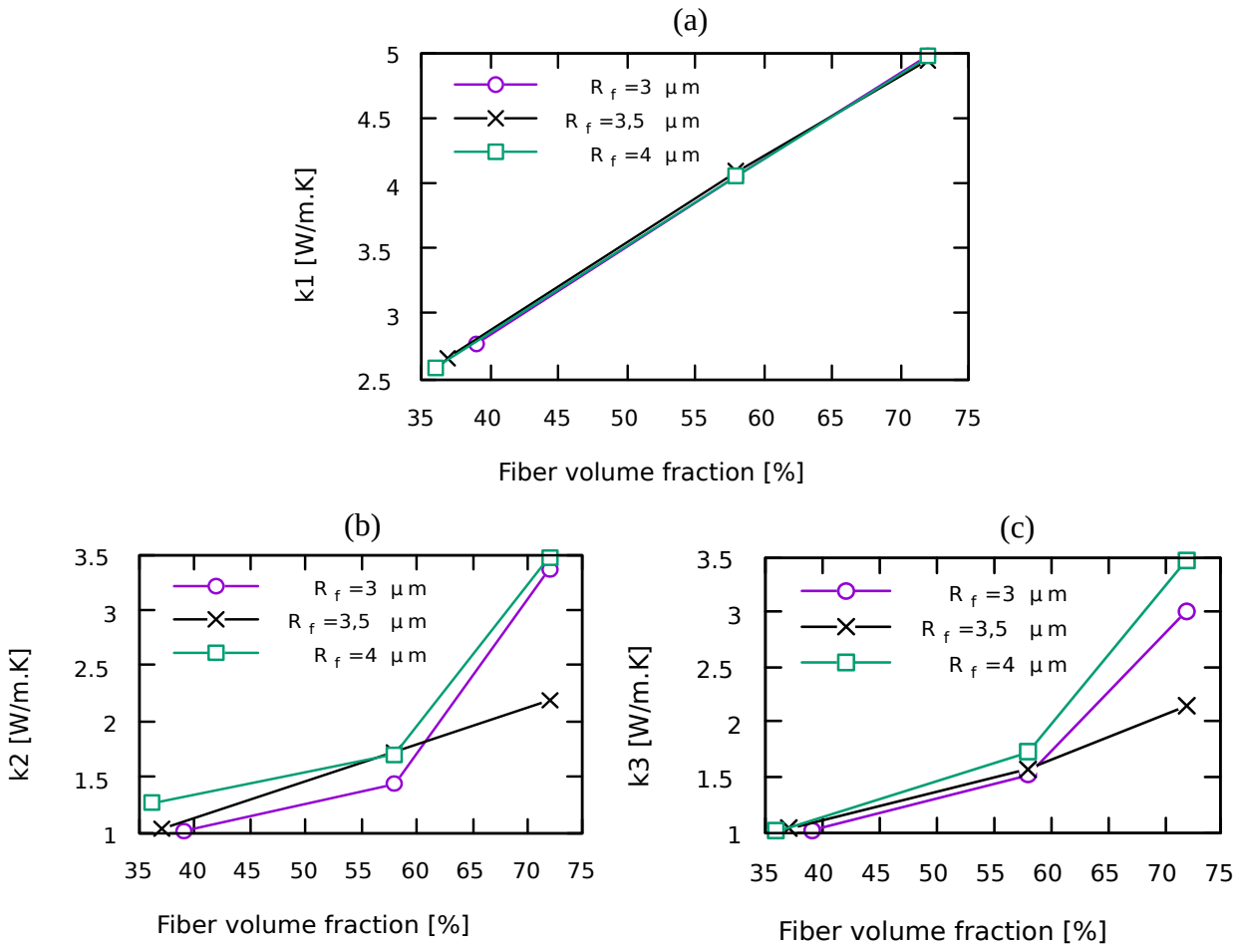

Figure 27: Effect of the fiber radius and volume fraction on the thermal conductivity of the CFR/ epoxy composite

However, if a transverse thermal gradient is imposed, the response in the same direction differs when the radius of the fibers is changed, which is well noticeable when a volume fraction of 72% of

carbon fibers is considered. This could be explained by the fact that the amount of the filler in the direction of the thermal loading is not the same with the different sizes considered even though the same amount of fibers is included in the whole unit cell. Indeed, the number and the localization of fibers in the direction of loading have been changed from one simulation to another according to each size in such a way to include the same volume fraction with different radii.

3.4.2.2.Fiber cross-section shape effect

In analogy to the mechanical study in section 3.2.3, an investigation of the effect of the shape of the fiber cross section on the thermal properties of the overall composite is carried out. Based on this, a comparison of circular fiber cross sections with elliptical ones is done.

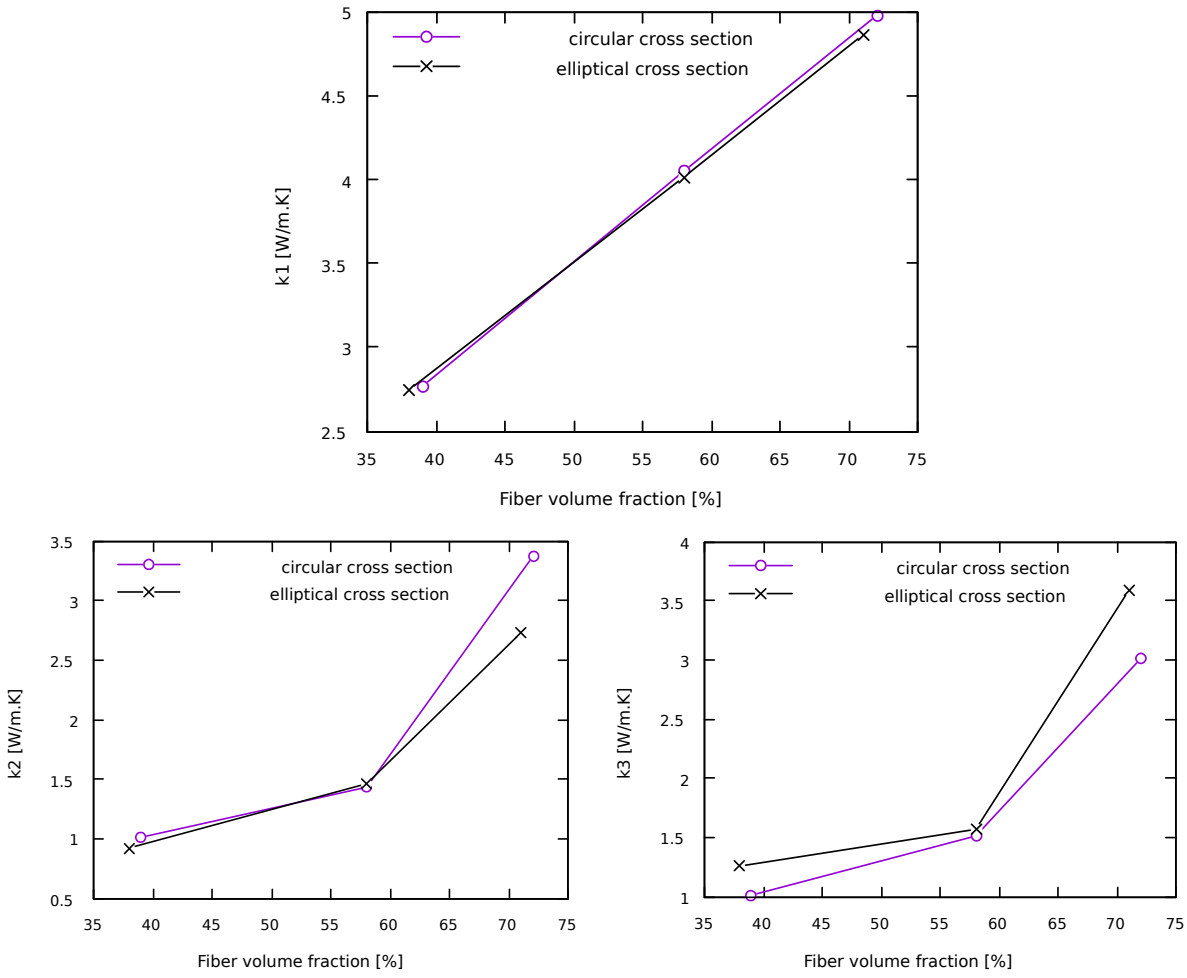

Figure 28: Effect of the shape of the cross section size and the volume fraction on the thermal conductivity of the CFR/epoxy composite

This comparison is illustrated in Fig. 28. The radius of the circular fibers considered in this investigation is 3 µm, while major and minor half axes of elliptical fibers cross section are 4 µm and 3 µm, respectively.

No effect has been observed when thermal loading has been imposed in the direction of fibers. The same thermal conductivity has been obtained for both shapes if the same fiber volume fraction is considered. However, the transverse thermal conductivities are not the same for all fiber volume fractions considered. This difference lies with the inequality of the fiber extension in the direction of thermal loading for both unit cells with different types of fibers.

3.4.3. Woven fiber composites

The unit cell used to simulate the thermal behavior of the woven glass-fiber-reinforced epoxy composite is shown in Fig. 29. Here the effect of the variation of the amount of reinforcing glass fibers is investigated. Since the undulations of the rovings is expected to be of minor importance, it has been neglected. The control of the volume fraction of rovings incorporated in the matrix has been performed by the variation of their dimensions (lateral thickness and vertical thickness).

Thermal conductivities k_1, k_2, k_3 obtained for each volume fraction are shown in Fig. 30. The values of k_1 and k_3 are identical, as expected, since they represent the thermal conductivities in the directions of the rovings. In contrast, k_2 represents the transverse thermal conductivity obtained through the application of a unidirectional macroscopic gradient of temperature in the normal direction of rovings. This latter shows a dramatic decrease by the incorporation of 18% of glass rovings into the epoxy matrix and then continues to decline slightly if a higher volume fraction of rovings is considered. A similar trend was found for k_1 and k_3, i.e., the higher the roving content the smaller is the heat conductivity of the overall composite. This was expected since the thermal conductivity of the glass fibers is much lower than the thermal conductivity of the epoxy matrix which could be also seen in Fig. 31, which shows a significant difference between the heat flux in both components of the composite, whose magnitude is much higher in the epoxy matrix. In conclusion, the mechanical reinforcement of the epoxy matrix by the inclusion of woven glass fibers comes with a considerable loss in terms of thermal conductivity. This loss could be compensated by the addition of a third filler with better thermal conductivity.

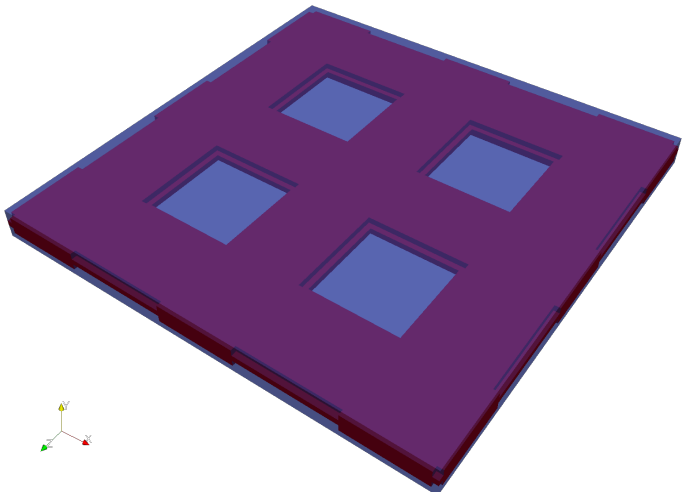

Figure 29: Unit cell considered to study the thermal behavior of woven glass fiber/epoxy composite

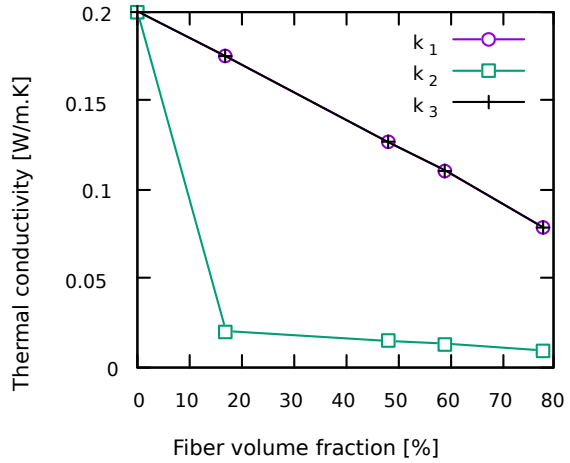

Figure 30: Effect of the fiber volume fraction on the thermal conductivity of the woven glass fiber/epoxy composite

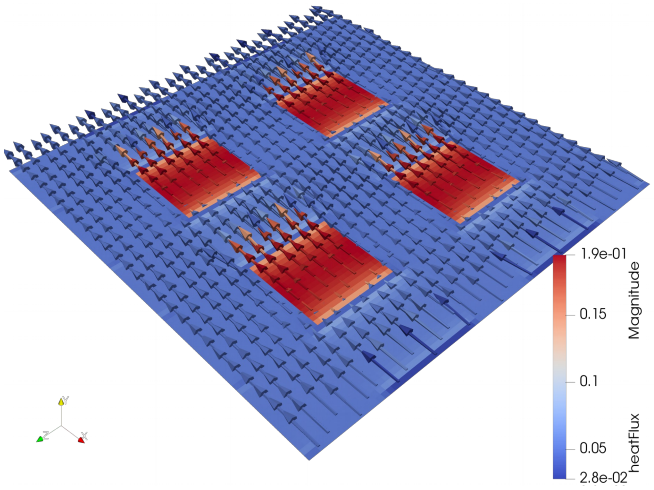

Figure 31: Distribution of the heat flux within the woven glass fiber/epoxy composite

4. Conclusion

This work has been carried out within the framework of the “FlexGen”-project and involved two main goals, the first was the numerical modeling of the complex behavior of the composite materials of two generator components and the second was the identification of microstructural parameters leading to favorable material properties.

More precisely, the project aimed at the computer-aided estimation of overall properties (e.g. stiffness, strength, thermal conductivity) of the composite materials for different microstructures and loading conditions. The goal was to thus obtain a comprehensive picture of the microstructural influence on the properties of the respective composite materials in order to improve the understanding of the material and, based on this, identify a favorable material design.

The failure behavior of composite structures is complex and involves a range of damage phenomena dictated by several factors including loading conditions, constituent materials as well as microstructural parameters such as the volume fraction, the spatial distribution and the size of the reinforcement and matrix voids.

Therefore, a significant effort has been made to successfully build efficient models, reflecting the elastoplastic damage behavior of the aforementioned materials, and to investigate the effect of the manufacturing variability in these materials on application-specific performance parameters like stiffness or strength.

In this work, microscopic failure mechanisms were investigated by finite element simulations using a geometrically nonlinear isotropic elastoplasticity model couple with isotropic damage including gradient-extension. Simulations made use of a variational constitutive update algorithm based on the exponential map and an adaptive remeshing algorithm for a refined numerical resolution of the cracked regions.

Three composite microstructures were simulated and numerically characterized: core-shell rubber particle-reinforced epoxy, woven glass fiber-reinforced epoxy, and carbon fiber-reinforced epoxy which are materials of the generator components.

The computational studies consisted in the investigation of the effect of the microstructural parameters on the behavior of the material with the purpose of finding a combination enabling the achievement of a composite with improved performance.

Prior to the study, the model has been validated by a comparison of numerically predicted material properties, which were obtained through typical tensile tests carried out on appropriate material unit cells, with corresponding experimental material properties provided by the project partners. A good agreement has been found between calculated and measured parameters. This paved the way to move forward and to seek favorable overall composite properties based on the systematic variation of microstructural parameters of the numerical model.

For the woven roving-reinforced composite, the influence of roving geometry and material parameters was tested on a three-dimensional model of woven rovings embedded in a brittle matrix. It was demonstrated that a reduced vertical thickness of the rovings is beneficial for the resistance against crack initiation. Reducing the lateral thickness can help to increase the maximum admissible strain of the composite.

For the core-shell rubber particle reinforced composite, the influence of particle volume fraction, particle size and matrix material properties on the overall material properties was tested on a three-dimensional cubic model representing the unit cell of the matrix including spherical voids representative of cavitated reinforcing particles. Here, the stiffness and strength of the composite were decreased by increasing the volume fraction of the particles, while the amount of dissipated energy increased, which indicates an improved toughness of the material.

Interest has been also given to study the effect of particle size on the overall behavior and it was established that the incorporation of particles with radius 50nm could lead to a more pronounced improvement in terms of energy absorption capability.

The matrix properties, such as the energy release rate and the yield stress, have been also considered among the microstructural parameters whose variation could enhance or diminish the performance of the core-shell-rubber particle modified epoxy. It has been found that the energy release rate has no effect on the properties of the material while the increase of the yield stress leads to an increase of the material strength and energy absorption capability.

An unsuccessful attempt has been made with the aim of analyzing the fracture toughness in presence of core-shell-particles in the matrix which required the modeling of a preexisting crack. A more realistic approach would involve the consideration of a multi-scale model, which wasn’t possible due to time constraints and is still subject of current research.

The investigation of the microstructure’s properties on the behavior of the carbon fiber-reinforced epoxy, being used in the rotor cap, included the consideration of several parameters relating to both components fibers and matrix. For example, two cross-section shapes (circular and elliptical) have been considered in the unit cell specific to this composite and two volume fractions of fibers (50% and 60%) have been tested. Matrix defects being a decisive factor in the assessment of the behavior of the composite, have been carefully studied. These defects were depicted by cylindrical voids with different volume fractions, different diameters and different distributions.

The analysis of the transversely isotropic behavior of this composite for different microstructural morphologies involved the conduction of various typical tensile and shear tests (longitudinal, transverse and in-plane shear tests) which enabled the investigation of the effect of the variation of the microstructural parameters on the effective material properties. The first key finding from this investigation is that fibers with elliptic cross section are better reinforcing agents than fibers with circular cross section. The second interesting finding is that CFRP with 50% of fibers exhibits a better energy absorption capability than CFRP with 60% fibres. However a decrease in the fiber amount leads to a decrease in the stiffness and the strength of the overall composite. Therefore the

selection of this parameter definitely depends on the required application-specific requirements. Results obtained from the simulation of the tensile response of the composite unit cell including voids were unexpected. It has been found that voids up to a specific amount could increase the energy absorption capability. This amount here is 8%. However to ensure this improvement, void clustering should be avoided.

In conclusion, for the three materials, there is a compromise to be achieved and a balance to be established such that all the microstructural parameters selected lead to the application specific reliability. Results obtained from multivariate analyses relating to both materials (carbon fiber-reinforced epoxy and core-shell-rubber particle-reinforced epoxy) have been gathered in Tables 12 and 15. For comparison, the proterties of the related defect-free materials are given in Tables 13 and 14. These tables represent a useful reference to select microstructural parameters considered in this study relating to each material, based on requirements in terms of mechanical performance. Thus, a clear picture about the effect of the investigated microstructural influence on the overall behavior of the composites has been successfully built.

Table 12: Micro-structural variability effect on the properties of the core-shell-rubber particle modified epoxy

Microstructural parameter	Parameter variation	Effect on:		
		Tensile stiffness	Tensile strength	Absorbed Energy
(Porosity, radius of pores)	(3.5%,50nm)	-6,4%	-5,36%	+95,2%
	(7.5%,50nm)	-13,1%	-10,6%	+109,8%
	(11.2%,50nm)	-18,45%	-14,8%	+244%
	(3.6%,25nm)	-6,9%	-5,23%	+95,2%
	(8%,25nm)	-13,9%	-10,6%	+171,5%
	(11.2%,25nm)	-18,5%	-14,7%	+156,8%
Energy release rate of the matrix Radius of pores=25nm Porosity=8%	70 J/m^2	0%	0%	0%
	90 J/m^2	0%	0%	0%
Yield stress of the matrix Radius of pores=25nm Porosity=8%	100 Mpa	0%	+24,4%	+5,4%
	120 Mpa	0%	+48,6%	+2,7%

Table 13: Material properties of the unmodified epoxy matrix of the core shell rubber-reinforced composite

Young's Modulus *E* (Mpa)	Initial Yield stress σ_{y0} (Mpa)	Elastic energy release rate g_c^e (J/m^2)	Absorbed energy ($Mpa.\mu m^3$)
2970	80,2	50	0.1363

Table 14: Material properties of a typical carbon fiber-reinforced composite without defects

Cross section shape of the fibers	circular
Volume fraction of fibers	60%
Longitudinal Young's modulus	143480 (Mpa)
Transverse Young's modulus	6687 (Mpa)
Shear modulus	3640 (Mpa)
Transverse strength	97.9 (Mpa)
Absorbed energy under transverse loading	0,63 (Mpa)
Absorbed energy under in-plane shear loading	0,64 (Mpa)

Microstructural parameter	Parameter variation	Effect on:						
		E_{11}	E_{22}	G_{12}	σ_{22}	σ_{12}	Absorbed Energy under Transverse Loading	Absorbed Energy under In-plane shear Loading
Cross section shape of fibers	Elliptic	+1,3%	+9%	+11,5%	+2,5%	+18%	+11%	+61%
Fiber volume fraction	50%	-11,9%	-11,5%	-17,9%	-1%	-7%	+58,7%	+17,18%
Porosity	2%		-6,7%		-11,3%		+35%	
	4%		-15,6%		-23,6%		+28,7%	
	8%		-22,5%		-32,4%		+21,85%	
	10%		-26,2%		-37,7%		-47,6%	
	14%		-36,3%		-40,8%		-52,45%	
Voids diameter (porosity =2%)	1µm		-6,7%		-11,3%		+35%	
	1.5µm		-7,3%		-13,3%		+16,5%	
Voids distribution (porosity =2%)	Well distributed		-6,7%		-11,3%		+35%	
	Accumulated		-3%		-10,1%		-54,1%	

Table 15: Micro-structural variability effect on the properties of the carbon fiber-reinforced epoxy

5. Appropriateness of work, usability of results and publications

5.1. Appropriateness of the work done

The subject of this project was the development of three-dimensional simulation models for materials to be used in the generators of conventional power plants. The work was necessary to achieve both, an improvement of the understanding of the involved materials and the identification of favorable material designs being tailored for the application at hand.

The behavior of the epoxy resin differs significantly from the macroscopic behavior on small scales, where unexpected large elastoplastic deformations can occur. In order to model the examined materials in a realistic manner, a suitable material model had to be developed and implemented and the associated finite element technology had to be adapted accordingly. This also involved an adaptive remeshing algorithm with the aim of increasing the numerical resolution of microscopic cracks. This was necessary in order to conduct the required simulations in a realistic manner within the limited project timeline.

An extensive campaign of three-dimensional finite-element simulations was necessary for the investigation of the influence of important system parameters on the elastoplastic deformation behavior as well as on the strength-relevant and thermal properties of the above-mentioned material systems. Some of the varied key parameters are listed below:

- volume fraction and size of the reinforcing elements (particles and fibers)
- geometry of the fibers and the rovings
- mechanical properties of the epoxy resin
- portions of pores as important material defects
- thermal conductivities of the base materials

The simulations were needed to understand and to characterize the influence of the above parameters on relevant properties of the composite materials, like yield strength, energy dissipation capability or thermal conductivity. Further, these investigations were needed for the identification of favorable parameters for the material design with the primary goal of increasing the load-bearing capacity. It is confirmed that the expenditure was necessary and economical and that the information corresponds to the books and, if applicable, the receipts.

5.2. Usability of results

Based on the project results, the above-mentioned composite materials could be examined virtually and advantageous material designs could be derived. As a result, an improvement in the

understanding of the materials could be achieved without the use of cost-intensive experiments. It was shown that the developed scientific methods can predict the properties with reasonable accuracy and correctly predict the influences of the system parameters on the effective material behavior.

The developed mathematical models and their implementation can be applied to numerous materials and thus have a high potential for the use in other scientific and industrial applications. Corresponding publications also enable the use by third parties. Future projects at Kiel University will also benefit from the experience and will be able to continue using the algorithms (material model, adaptive remeshing) and results.

5.3. Publications related to the project

The following overview lists the scientific publications which resulted from the project:

Nguyen, T.T., Wulfinghoff, S. and Reese, S., 2018. Micromechanical Modeling of a Generator Stator Electrical Insulation System. *PAMM*, *18*(1), p.e201800328.

Nguyen, T.T., Fassin, M., Eggersmann, R., Reese, S. and Wulfinghoff, S., 2020. Gradient-extended brittle damage modeling. *Technische Mechanik – European Journal of Engineering Mechanics*, *40*(1), pp.53-58.

Boussetta, H., Dittmann, J., Wulfinghoff, S., 2021. Application of a geometrically nonlinear elastoplastic gradient-enhanced damage model with incremental potential to composite microstructures. Accepted for publication in *Archives of Mechanics*.

The following overview lists the scientific publications which are associated to the project:

Fassin, M., Eggersmann, R., Wulfinghoff, S. and Reese, S., 2019. Gradient-extended anisotropic brittle damage modeling using a second order damage tensor-theory, implementation and numerical examples. *International Journal of Solids and Structures*, *167*, pp.93-126.

Fassin, M., Eggersmann, R., Wulfinghoff, S. and Reese, S., 2019. Efficient algorithmic incorporation of tension compression asymmetry into an anisotropic damage model. *Computer Methods in Applied Mechanics and Engineering*, *354*, pp.932-962.

References

Bagheri, R., Marouf, B. T., Pearson, R. A., 2009. Rubber-toughened epoxies: A critical review. Polymer Reviews 49 (3), 201-225.

Boussetta, H., Dittmann, J., Wulfinghoff, S., 2021. Application of a geometrically nonlinear elastoplastic gradient-enhanced damage model with incremental potential to composite microstructures. Submitted.

Gao, G., Li, Y., 2016. Mechanical properties of woven glass-fiber reinforced polymer composites. Emerging Materials Research 5, 201-2018.

Garg, A. C., Mai, Y.-W., 1988. Failure mechanisms in toughened epoxy resins – A review. Composites Science and Technology 31 (3), 179-223.

Giannakopoulos, G., Masania, K., Taylor, A. C., 2011. Toughening of epoxy using core-shell particles. Journal of Materials Science 46, 327-338.

Huang, Y., Kinloch, A. J., 1992. Modelling of the toughening mechanisms in rubber-modified epoxy polymers. Journal of Materials Science 27, 2763-2769.

Jacob, G. C., Starbuck, J. M., Fellers, J. F., Simunovic, S., 2005. Effect of fiber volume fraction, fiber length and fiber tow size on the energy absorption of chopped carbon fiber. Polymer Composites 26, 293.305.

Manzione, L. T., Gillham, J. K., McPherson, C. A., 1981. Rubber-modified epoxies. I. Transitions and morphology. Journal of Applied Polymer Science 26 (3), 889-905.

Mehdikhani, M., Gorbatikh, L., Verpoest, I. and Lomov, S. V., 2019. Voids in fiber-reinforced polymer composites: A review on their formation, characteristics, and effects on mechanical performance. *Journal of Composite Materials*, *53* (12), 1579-1669.

Meijer, H. E. H., Govaert, L. E., 2003. Multi-scale analysis of mechanical properties of amorphous polymer systems. Macromolecular Chemistry and Physics 204 (2), 274-288.

Muritiba, A. E. F., 2010. Algorithms and models for combinatorial optimization problems. PhD Thesis, Alma Mater Studiorum Universita di Bologna

Park, S.-J., Seo, M.-K., Shim, H.-B., Rhee, K.-Y., 2004. Effect of different cross-section types on mechanical properties of carbon fibers-reinforced cement composites. Materials Science and Engineering A 366 (2), 348-355.

Pijnenburg, K. G. W., Van der Giessen, E., 2001. Macroscopic yield in cavitated polymer blends. International Journal of Solids and Structures 38 (20), 3575-3598.

Rajak, D. K., Pagar, D. D., Menezes P. L., Linul, E., 2019. Fiber-reinforced polymer composites: Manufacturing, properties, and applications. Polymers 11 (10), 1667.

Seymour, R. B., 1989. Origin and Early Development of Rubber-Toughened Plastics. Ch. 1 in Rubber-Toughened Plastics, 3-13.

Smit, R. J. M., Brekelmans, W. A. M., Meijer, H. E. H., 1999. Prediction of the large-strain mechanical response of heterogeneous polymer systems: local and global deformation behaviour of a representative volume element of voided polycarbonate. Journal of the Mechanics and Physics of Solids 47 (2), 201-221.

Steenbrink, A. C., Van der Giessen, E., 1999. On cavitation, post-cavitation and yield in amorphous polymer-rubber blends. Journal of the Mechanics and Physics of Solids 47 (4), 843-876.

Taylor, R. L., 2014. FEAP - finite element analysis program. URL http://www.ce.berkeley/feap

Yee, A. F., Pearson, R. A., 1986. Toughening mechanisms in elastomer-modified epoxies: Part 1 mechanical studies. Journal of Materials Science 21, 2462-2474.

Yoon, S.H., Takano, N., Korai, Y., Mochida, I., 1997. Crack formation in mesophase pitch-basedcarbon fibres: Part I Some influential factors for crack formation. Journal of Materials Science 32, 2753-2758.

Berichtsblatt

1. ISBN oder ISSN geplant	2. Berichtsart (Schlussbericht oder Veröffentlichung) Schlussbericht

3. Titel
Report
03ET7087E
Project: FlexGen – Innovations for the development of turbo generators for the support of the energy revolution
Subproject: Computer-aided prediction and optimization of the thermal and mechanical properties of novel composite materials for generator components with special focus on strength- and endurance-relevant properties

4. Autor Wulfinghoff, Stephan	5. Abschlussdatum des Vorhabens März 2021
	6. Veröffentlichungsdatum geplant
	7. Form der Publikation Technische Informationsbibl. (TIB)
8. Durchführende Institution(en) (Name, Adresse) Christian-Albrechts-Universität zu Kiel Institut für Materialwissenschaft Computational Materials Science Kaiserstr. 2 24143 Kiel Germany	9. Ber. Nr. Durchführende Institution 1
	10. Förderkennzeichen 03ET7087E
	11. Seitenzahl 58
12. Fördernde Institution (Name, Adresse) Bundesministerium für Wirtschaft und Energie (BMWi) 53107 Bonn	13. Literaturangaben 24
	14. Tabellen 15
	15. Abbildungen 31

16. Zusätzliche Angaben
-

17. Vorgelegt bei (Titel, Ort, Datum)
-

18. Kurzfassung
Im Projekt FlexGen wurden partikel- und faserverstärkte Verbundwerkstoffe für den Bau von Generatoren untersucht, die in konventionellen Kraftwerken eingesetzt werden. Diese neuen Werkstoffe sind erforderlich, um eine sichere Anwendung unter Berücksichtigung geänderter Beanspruchungszyklen infolge der Energiewende zu gewährleisten. Für ein umfassendes Werkstoffverständnis ist die Vorhersage von plastischen Verformungen und Rissausbreitungsmechanismen in der Mikrostruktur der Verbundwerkstoffe durch realistische und effiziente Materialmodelle erforderlich. Dies ist Gegenstand aktueller Forschungsarbeiten und wurde zuvor nicht auf die in diesem Projekt anvisierten Generatorkomponenten angewandt. Die Zielsetzung dieses Teilvorhabens war es, ein möglichst umfassendes Bild des Einflusses der Werkstoffmikrostrukturen auf die Eigenschaften des jeweiligen Verbundwerkstoffes gewinnen, um das Werkstoffverständnis zu verbessern und darauf aufbauend ein für die oben genannte Anwendung vorteilhaftes Werkstoffdesign zu erreichen. Dazu wurde ein neues mathematisches Materialmodell entwickelt und implementiert, mit dem mikroskopische Versagensmechanismen in dreidimensionalen numerischen Modellen der Verbundmikrostrukturen untersucht wurden. Das Modell wurde verwendet, um Einblicke in das mikroskopische Versagen eines spröden gewebten Verbundmaterials, eines partikelverstärkten Kunststoffs und eines kohlenstofffaserverstärkten Verbunds zu geben. Der Einfluss unterschiedlicher Struktur- und Materialparameter auf das mechanische und thermische Verhalten wurde charakterisiert. Dadurch wurde das Verständnis des mikrostrukturellen Einflusses auf das Werkstoffverhalten signifikant verbessert. So konnten Hinweise für das Werkstoffdesign sowie vorteilhafte Designparameter abgeleitet werden. Die entwickelten und veröffentlichten mathematischen Modelle und deren Implementierungen lassen sich auf zahlreiche Materialien anwenden und haben somit ein hohes Potenzial für den Einsatz in anderen wissenschaftlichen und industriellen Anwendungen. Auch zukünftige Projekte der CAU werden von den Erfahrungen profitieren und die Algorithmen und Ergebnisse weiter nutzen können.

19. Schlagwörter
Energiewende, Verbundwerkstoffe, Materialwissenschaft, Simulation, Schädigung

20. Verlag Technische Informationsbibliothek (TIB)	21. Preis 0 €